

C.P. No. 291
(18,062)
A.R.C. Technical Report

C.P. No. 291
(18,062)
A.R.C. Technical Report



MINISTRY OF SUPPLY

AERONAUTICAL RESEARCH COUNCIL
CURRENT PAPERS

**The Use of Multiple
Diaphragms in Shock Tubes**

By

B. D. Henshall, Ph.D.

LIBRARY
ROYAL AIR FORCE ESTABLISHMENT
BELFORD.

LONDON . HER MAJESTY'S STATIONERY OFFICE

1956

SIX SHILLINGS NET

The Use of Multiple Diaphragms in Shock Tubes

- By -

B. D. Henshall, Ph.D.,
of the Aerodynamics Division, N.P.L.3rd December, 19551. SUMMARY

Calculations are presented which illustrate the advantages of various types of multiple-diaphragm shock tubes over the single-diaphragm conventional shock tube. Shock tubes having a discontinuous change of cross-section at a diaphragm station or at any other position along the tube are also considered.

2. Notation

a	velocity of sound
A	cross-sectional area of shock tube
C_p	specific heat at constant pressure
C_v	specific heat at constant volume
M	Mach number
n	number of diaphragms in a multiple-diaphragm shock tube
p	absolute pressure
R	the gas constant
t	time
T	absolute temperature
u	flow velocity
U	shock velocity; subscript corresponds to flow region <u>ahead</u> of the shock
x	distance measured along longitudinal axis of shock tube
γ	C_p/C_v , the ratio of the specific heats
$\phi_1 \phi_2 \phi_3$	functions of shock Mach number M_s (see equations (5.9), (5.10) and (5.12)).

G/

- G the gain factor (see Section 7.1)
- $M()$ flow Mach number with respect to the local speed of sound (e.g., $M_2 = \frac{u}{a_2}$)
- $M_{S()}$ shock wave propagation Mach number with respect to the speed of sound in the flow ahead of the shock front (e.g., $M_{S_1} = U_1/a_1$)
- P_S pressure ratio across a shock wave (> 1)
- $P_I \left(= P_o^{\frac{1}{n}} \right)$ the individual pressure ratio across each diaphragm of a multiple-diaphragm shock tube
- P_o overall pressure ratio across extreme ends of any type of shock tube
- T_o overall temperature ratio across extreme ends of any type of shock tube

Subscripts

1,2,3,4,5 etc. identify quantities related to gas in corresponding region of shock tube flow (see Figures)

Special Non-Dimensional Notation

$$P_{mn} = \frac{P_m}{P_n} \quad \text{a pressure ratio}$$

$$T_{mn} = \frac{T_m}{T_n} \quad \text{a temperature ratio}$$

3. Introduction

During the past decade the shock tube has become accepted as a tool of aerodynamic research: the extreme versatility of shock tube installations has led to their use for the investigation of a variety of gas-dynamic problems. Increasing interest in hypersonic research has stimulated the development of special 'hypersonic shock tubes'. These offer a comparatively simple method whereby very high Mach number flows - with stagnation temperatures approximating to those of full-scale flight - may be generated. In order to operate hypersonic shock tubes satisfactorily, it is necessary to produce shock waves which are considerably stronger than the strongest obtainable from a simple 'conventional' shock tube.

Ref. 1 contains a resumé of the aerodynamic principles involved in the production of very strong shock waves and very high Mach number flows in hypersonic shock tubes; in particular, the 'double-diaphragm' technique, which increases the maximum attainable shock strength for a given overall pressure ratio across the extreme ends of the shock tube, is discussed in a preliminary manner. In the present paper, the concept of a multiple-diaphragm shock tube is considered in greater detail; and several types of double- and multiple-diaphragm shock tubes are

discussed/

discussed and their performance evaluated. For completeness, consideration is also given to shock tubes having discontinuous changes of cross-section. General formulae have been derived which are applicable to any gas combination in any type of shock tube. For simplicity, these formulae have been evaluated for the particular case when γ , the ratio of the specific heats of the gases filling the shock tube, is constant and equal to 1.4 and when the initial temperature is constant throughout the shock tube; that is, $T_0 = 1$. In this manner the relative merits of the different types of multiple-diaphragm shock tubes are not confused by the effects of the use of different gases.

3.1 The Simple Shock Tube

Fig. 1 is a time-distance ($t - x$) diagram of simple shock tube flow and it illustrates the notation defined above in Section 2. The theory of the simple shock tube has been extensively treated^{2,3} and, in the present paper, equations obtained directly from such theory will be quoted without derivation. The initial pressure and temperature ratios, P_0 and T_0 respectively, across the diaphragm are related to the resultant shock Mach number M_{S_1} by the equation

$$P_0 = \left\{ \frac{2\gamma_1}{\gamma_1 + 1} M_{S_1}^2 - \frac{\gamma_1 - 1}{\gamma_1 + 1} \right\} \left\{ 1 - T_0^{-\frac{1}{2}} \left(\frac{\gamma_4 - 1}{\gamma_1 + 1} \right) \left(\frac{M_{S_1}^2 - 1}{M_{S_1}} \right) \right\}^{-\frac{2\gamma_4}{\gamma_4 - 1}}$$

.....(3.1)

where

$$P_0 = P_4/P_1 = P_{41}$$

and

$$T_0 = T_4/T_1 = T_{41} \quad \text{by definition.}$$

Equation (3.1) shows that, as $P_0 \rightarrow \infty$, the shock Mach number M_{S_1} approaches a limiting value, given by

$$M_{S_1} \simeq \frac{\gamma_1 + 1}{\gamma_4 - 1} T_0^{\frac{1}{2}} = \left(\frac{\gamma_1 + 1}{\gamma_4 - 1} \right) \frac{a_4}{a_1} \sqrt{\frac{\gamma_1}{\gamma_4}} \quad \text{.....(3.2)}$$

For large M_{S_1} , the gas in the chamber (region 4) must have a low molecular weight, a low γ_4 and as high a temperature as practicable. Equation (3.2) illustrates the advantage of heating the chamber gas and of using different gas combinations in a simple shock tube. As previously stated, the performance of multiple-diaphragm shock tubes will be evaluated only on the assumptions that $\gamma_1 = \gamma_4 = 1.4$ and $T_0 = 1$. For the simple shock tube, with arbitrary P_0 and T_0 , we have from (3.1), if $\gamma_1 = \gamma_4 = 1.4$,

$$P_0 = \left\{ \frac{7M_{S_1}^2 - 1}{6} \right\} \left\{ 1 - \frac{T_0^{-\frac{1}{2}}}{6} \left(\frac{M_{S_1}^2 - 1}{M_{S_1}} \right) \right\}^{-7} \quad \text{.....(3.3)}$$

From equation (3.3), values of P_0 were calculated for a range of values of T_0 (1 to 15 in unit steps) and an independent range of values of M_{S_1} (1 to 8 in 0.1 steps). The general results are displayed in Table I and Fig. 2. Note that, when P_0 is large (say $> 10^4$), a small increase of T_0 increases the attainable shock Mach number M_{S_1} appreciably, whereas a large increase of P_0 has only a small effect

on/

on M_{S_1} . Thus one convenient way to increase the attainable M_{S_1} for a given P_0 and the given initial condition $T_0 = 1$ is to introduce a device which effectively sacrifices pressure ratio P_0 in favour of increased temperature ratio T_0 : such a device is the multiple-diaphragm shock tube. [A detailed discussion of the flow processes occurring in these types of shock tubes is postponed to Section 4.1].

3.2 The Simple Shock Tube - A Special Case

Let us consider the simple shock tube flow pattern given in Fig. 1. With the exception of the acceleration region in the expansion wave, all the gas particles in the shock tube are at rest or in uniform motion with velocity $u_2 (= u_3)$ towards the end of the channel. Since the gas behind the shock has been compressed, its temperature T_2 is higher than T_1 ; and since the gas behind the rarefaction wave has been expanded, its temperature T_3 is lower than T_4 . Consequently, a discontinuity of temperature occurs at those coincident points in the uniform gas flow which were originally on either side of the diaphragm. This 'contact surface', or temperature discontinuity, causes the Mach number M_2 of the flow between the shock and the contact surface to be different from the Mach number M_3 of the flow between the contact surface and the rarefaction wave.

Clearly it is possible to choose T_4 and T_1 such that $T_2 = T_3$ and hence $M_2 = M_3$ if gases having the same γ were originally on either side of the diaphragm. Therefore, in theory, no contact surface would be present and the duration of quasi-steady flow would be increased. It should be noted that the flow in region 3 would be turbulent since it has passed through the remnants of the shattered diaphragm; however, in hypersonic shock tubes this 'steady' flow is expanded in a nozzle and hence fluctuations may be smoothed out to a satisfactory level. This possibility is worth experimental investigation since the duration of steady flow in a hypersonic shock tube is very limited¹.

The relations between P_0 , T_0 and M_{S_1} may be developed for the special case $M_2 = M_3$ by using the following equations of simple shock tube theory:-

$$\frac{T_4}{T_3} = \left(1 + \frac{\gamma_4 - 1}{2} M_3^2 \right)^2 \quad \dots\dots(3.4)$$

$$\frac{T_2}{T_1} = \frac{\left\{ \gamma_1 M_{S_1}^2 - \frac{\gamma_1 - 1}{2} \right\} \left\{ \frac{\gamma_1 - 1}{2} M_{S_1}^2 + 1 \right\}}{\left(\frac{\gamma_1 + 1}{2} \right)^2 M_S^2} \quad \dots\dots(3.5)$$

and
$$M_2 = (M_{S_1}^2 - 1) \left[\left\{ \gamma_1 M_{S_1}^2 - \frac{\gamma_1 - 1}{2} \right\} \left\{ \frac{\gamma_1 - 1}{2} M_{S_1}^2 + 1 \right\} \right]^{-\frac{1}{2}} \quad \dots\dots(3.6)$$

Now, put $M_2 = M_3$ and $T_2 = T_3$ (note that this implies $\gamma_4 = \gamma_1$ because $u_2 = u_3$ so that $a_2 = a_3$) and combine the above equations (3.4) to (3.6) to obtain:-

T/O

$$T_0 = T_{41} = T_{43} \cdot T_{32} \cdot T_{21}$$

$$= \left\{ \frac{2 \sqrt{\left(\gamma_1 M_{S_1}^2 - \frac{\gamma_1 - 1}{2} \right) \left(\frac{\gamma_1 - 1}{2} M_{S_1}^2 + 1 \right)} + (\gamma_1 - 1)(M_{S_1}^2 - 1)}{(\gamma_1 + 1)M_{S_1}} \right\}^2 \dots (3.7)$$

which, using (3.1), reduces to

$$P_0 = \left\{ \frac{2\gamma_1}{\gamma_1 + 1} M_{S_1}^2 - \frac{\gamma_1 - 1}{\gamma_1 + 1} \right\} \left[1 + \frac{(M_{S_1}^2 - 1)}{\frac{\gamma_1 - 1}{\gamma_1 + 1} \sqrt{\left(\gamma_1 M_{S_1}^2 - \frac{\gamma_1 - 1}{2} \right) \left(\frac{\gamma_1 - 1}{2} M_{S_1}^2 + 1 \right)}} \right]^{\frac{2\gamma_1}{\gamma_1 - 1}} \dots (3.8)$$

If $\gamma_4 = \gamma_1 = 1.4$, (3.7) and (3.8) become

$$T_0 = \left[\frac{\sqrt{(7M_{S_1}^2 - 1)(M_{S_1}^2 + 5)} + (M_{S_1}^2 - 1)}{6M_{S_1}} \right]^2 \dots (3.9)$$

and

$$P_0 = \left[\frac{7M_{S_1}^2 - 1}{6} \right] \left[1 + \frac{(M_{S_1}^2 - 1)}{\sqrt{(7M_{S_1}^2 - 1)(M_{S_1}^2 + 5)}} \right]^7 \dots (3.10)$$

Hence, using M_{S_1} as a parameter, a unique curve of P_0 versus T_0 can be derived from equations (3.9) and (3.10) for the 'constant Mach number' shock tube. Calculated results are given in Table II and plotted in Fig. 2. It is pertinent to note that in order to produce strong shock waves T_0 must be considerably larger than the values normally employed in simple shock tubes. Fortunately, the multiple diaphragm technique reduces this difficulty and further consideration of this 'constant Mach number' shock tube is accordingly deferred to Section 6.1.

4. The Double Diaphragm Shock Tube - Reflected Shock Type

The reflected shock type of double-diaphragm shock tube is shown in Fig. 3; the primary shock $M_{S_6}^*$, which is produced by the rupture of diaphragm D_1 , undergoes normal reflection at diaphragm D_2 and leaves the gas in region 4 at rest at an increased temperature and pressure (with respect to its initial state in region 6). After a predetermined delay, diaphragm D_2 is ruptured and the ensuing flow produces a shock M_{S_1} , where $M_{S_1} > M_{S_6}$. Let us compare the shock Mach numbers produced in a double-diaphragm shock tube and in the equivalent single-diaphragm shock tube having the same overall temperature and pressure ratios. In the double-diaphragm case, the pressure and temperature ratios across the second diaphragm D_2 are p_{41} and T_{41} and in the equivalent single-diaphragm case those ratios are p_{21} and T_{21} respectively. Now the reservoir upstream of diaphragm D_2 has a

pressure/

*It is convenient to label a shock with its corresponding shock Mach number.

pressure p_4 ($< p_3$) and a temperature T_4 ($> T_3$) due to the reflection of the primary shock $M_{S_6}^*$; and since we have previously noted that a device which sacrifices pressure ratio for increased temperature ratio will produce an increase of shock Mach number, it follows that M_{S_1} is greater than the corresponding value for a single-diaphragm shock tube.

4.1 The Reflection of a Normal Shock Wave from a Rigid Wall

Before complete calculations can be made of the performance of the reflected shock type of double-diaphragm shock tube, the relations between the pressure and temperature in the reservoir (region 4 of Fig. 3) and the original conditions in the double-diaphragm chamber (region 6) must be determined. Now, from shock wave theory

$$p_{46} = \left\{ \frac{2\gamma_6}{\gamma_6 + 1} M_{S_6}^2 - \frac{\gamma_6 - 1}{\gamma_6 + 1} \right\} \left\{ \frac{(3\gamma_6 - 1) M_{S_6}^2 - 2(\gamma_6 - 1)}{(\gamma_6 - 1) M_{S_6}^2 + 2} \right\} \dots\dots(4.1)$$

$$\text{and } T_{46} = \frac{\{(3\gamma_6 - 1) M_{S_6}^2 - 2(\gamma_6 - 1)\} \{2(\gamma_6 - 1) M_{S_6}^2 + (3 - \gamma_6)\}}{(\gamma_6 + 1)^2 M_{S_6}^2} \dots\dots(4.2)$$

When $\gamma_6 = 1.4$, (4.1) and (4.2) become

$$p_{46} = \left[\frac{7M_{S_6}^2 - 1}{6} \right] \left[\frac{8M_{S_6}^2 - 2}{M_{S_6}^2 + 5} \right] \dots\dots(4.3)$$

$$\text{and } T_{46} = \frac{(4M_{S_6}^2 - 1)(M_{S_6}^2 + 2)}{9M_{S_6}^2} \dots\dots(4.4)$$

From (4.3) and (4.4) calculations of p_{46} and T_{46} were made for a range of M_{S_6} from 1 to 8 in 0.1 steps and the results are reproduced as Table III.

4.2 Effect of Variation of Intermediate Double-Diaphragm Chamber Pressure (p_6 - Fig. 3)

Let us refer to Fig. 3 and suppose the overall pressure ratio across the extreme ends of the tube $P_0 = p_{61} = 10^4$ and the initial temperature is constant throughout the tube, that is, $T_0 = 1$. From Table I we note that the shock Mach number M_{S_1} corresponding to $P_0 = 10^4$, $T_0 = 1$ and a single diaphragm shock tube is 3.85. Now consider the effect of the insertion of the second diaphragm D_2 and the variation of the intermediate pressure p_6 . For example, let $p_{61} = 10^2$. Then p_{66} is known since

$$P_0 = p_{66} \cdot p_{61} = 10^4.$$

The corresponding shock Mach number M_{S_6} ($= 2.370$) is found from the general ($P_0 - T_0$) Table I. Then p_4 and T_4 are found from the general reflected shock Table III; the numerical values are $p_{46} = 25.25$ and $T_{46} = 3.236$. Now $p_{41} = p_{46} \cdot p_{61}$ is determined, and the final shock Mach number M_{S_1} ($= 5.22$) is obtained

by/

*See equations (4.3), (4.4) and Table III.

by a further interpolation* from Table I. This procedure may be repeated for values of p_6 ranging from p_0 to p_1 ; similar calculations may be made for other values of P_0 . Fig. 4 reproduces the results of these calculations and it is clear that a considerable increase in the attainable shock Mach number is possible by a suitable choice of the intermediate pressure ratio p_{61} .

5. The Double-Diaphragm Shock Tube - Unsteady Expansion Type

Instead of rupturing the second diaphragm D_2 by an external agency after the full reflected shock pressure p_4 is reached upstream of the diaphragm as in Fig. 3; it is possible to make the diaphragm D_2 so weak that it bursts immediately when the shock M_{s6} strikes it. A distance-time diagram for this second type of double-diaphragm shock tube⁴ flow is given in Fig. 5. Shock M_{s6} shatters diaphragm D_2 on impact, and the pressure ratio p_4 , (related to p_{61} and M_{s6}) across the rarefaction wave accelerates the flow, in particular $M_{s4} > M_{s1}$. A relation is required between M_{s6} , p_{61} and M_{s4} . The relevant equations, obtained from the theory of the simple shock tube, are:-

From the normal shock equations:-

$$p_{46} = \left\{ \frac{2\gamma_6}{\gamma_6 + 1} M_{s6}^2 - \frac{\gamma_6 - 1}{\gamma_6 + 1} \right\} \dots\dots(5.1)$$

$$p_{21} = \left\{ \frac{2\gamma_1}{\gamma_1 + 1} M_{s1}^2 - \frac{\gamma_1 - 1}{\gamma_1 + 1} \right\} \dots\dots(5.2)$$

$$\frac{u_3}{a_1} = \frac{u_2}{a_1} = \frac{2}{\gamma_1 + 1} \left[M_{s1} - \frac{1}{M_{s1}} \right] \dots\dots(5.3)$$

$$\frac{u_4}{a_6} = \frac{2}{\gamma_6 + 1} \left[M_{s6} - \frac{1}{M_{s6}} \right] \dots\dots(5.4)$$

$$M_{s4} = (M_{s6}^2 - 1) \left\{ \frac{\gamma_6}{2} M_{s6}^2 - \frac{\gamma_6 - 1}{2} \right\} \left\{ \frac{\gamma_6 - 1}{2} M_{s6}^2 + 1 \right\}^{-\frac{1}{2}} \dots\dots(5.5)$$

and from the rarefaction wave equations:-

$$p_{43} = \frac{\gamma_6 - 1}{2\gamma_6} = \frac{1 + \frac{\gamma_6 - 1}{2} M_3^2}{1 + \frac{\gamma_6 - 1}{2} M_4^2} \cdot u_{43} \dots\dots(5.6)$$

[Note that $\gamma_6 = \gamma_4 = \gamma_3$ and $\gamma_2 = \gamma_1$].

Now/

*See Appendix I.

Now, since $p_2 = p_3$,

$$p_{43} = p_{46} \cdot p_{61} \cdot p_{12} = \left[1 + \frac{\gamma_6 - 1}{2} M_3 \right]^{2\gamma_6 / \gamma_6 - 1} \cdot \left[1 + \frac{\gamma_6 - 1}{2} M_4 \right]^{2\gamma_6 / \gamma_6 - 1} \dots (5.7)$$

hence, using (5.1), (5.2) and (5.5),

$$p_{61} \cdot \phi_1 = \phi_2 \dots (5.8)$$

where $\phi_1 = \left[\frac{2\gamma_6}{\gamma_6 + 1} M_{S_6}^2 - \frac{\gamma_6 - 1}{\gamma_6 + 1} \right] \left[1 + \frac{\gamma_6 - 1}{2} M_4 \right]^{2\gamma_6 / \gamma_6 - 1} \dots (5.9)$

and $\phi_2 = \left[\frac{2\gamma_1}{\gamma_1 + 1} M_{S_1}^2 - \frac{\gamma_1 - 1}{\gamma_1 + 1} \right] \left[1 + \frac{\gamma_6 - 1}{2} M_3 \right]^{2\gamma_6 / \gamma_6 - 1} \dots (5.10)$

Also, from (5.3), (5.4) and (5.6), after some reduction, it follows that

$$1 + \frac{\gamma_6 - 1}{2} M_3 = \left\{ 1 - \frac{\gamma_6 - 1}{2} \frac{\gamma_6 + 1}{\gamma_1 + 1} \frac{a_1}{a_6} \left[\frac{M_{S_1}^2 - 1}{M_{S_1}} \right] \frac{1}{\phi_3} \right\}^{-1} \dots (5.11)$$

where $\phi_3 = \left\{ \frac{M_{S_6}^2 - 1}{M_{S_6}} \right\} \left\{ \frac{1 + \frac{\gamma_6 - 1}{2} M_4}{M_4} \right\} \dots (5.12)$

Now, from (5.5), M_4 is known for a given M_{S_6} and hence ϕ_1 and ϕ_3 are calculable for the given value of M_{S_6} . Values of ϕ_1 and ϕ_3 are presented in Table IV for a range of M_{S_6} values from 1 to 8 in 0.1 steps. Then, from (5.10) and (5.11) it follows that

$$p_{61} \phi_1 = \phi_2 = \left\{ \frac{2\gamma_1}{\gamma_1 + 1} M_{S_1}^2 - \frac{\gamma_1 - 1}{\gamma_1 + 1} \right\} \left\{ 1 - \frac{\gamma_6 - 1}{2\gamma_6} \frac{\gamma_6 + 1}{\gamma_1 + 1} \frac{a_1}{a_6} \left[\frac{M_{S_1}^2 - 1}{M_{S_1}} \right] \right\}^{-2\gamma_6 / \gamma_6 - 1} \dots (5.13)$$

If (5.13) is compared with (5.1) it is seen that the equations are of the same form and hence their solutions are similar; in particular M_{S_1} is the same as for a single-diaphragm shock tube in which

$$P_0 = \phi_2 \dots (5.14)$$

and/

and
$$\left(\frac{\gamma_4 - 1}{\gamma_4 + 1}\right) T_0^{-1/2} = \frac{\gamma_0 - 1}{2\zeta_3} \frac{\gamma_0 + 1}{\gamma_1 + 1} \frac{a_1}{a_3} \dots (5.15)$$

Although the R.H.S. of equation (5.15) enables the effects of the use of different gases in regions 1 and 6 of Fig. 5 to be evaluated, only the simple case when $\gamma_0 = \gamma_1 = 1.4$ and $a_3 = a_1$ is considered here.

Then T_0 is equivalent to $\frac{25}{36} \phi_3^2$ and P_0 is equivalent to ϕ_2 .

Thus it is possible to calculate the performance of the unsteady expansion type of double-diaphragm shock tube and to investigate the effects of variation of the intermediate chamber pressure p_6 for a given overall pressure ratio P_0 . A specimen calculation follows.

Refer to Fig. 5, and suppose $P_0 = p_{7,1} = 10^4$ and that $T_0 = 1$. Then, if $p_{6,1} = 10^3$ is assumed, it follows that $p_{7,6}$ is known since $P_0 = p_{7,6} p_{6,1} = 10^4$. The corresponding shock Mach number $M_{S_6} (= 2.370)$ is found from the general $(P_0 - T_0)$ Table I and ϕ_1 and ϕ_3 are determined, corresponding to $M_{S_6} = 2.370$, from Table IV, so that $\phi_2 = \phi_1 p_{6,1}$ is known and thus the equivalent

$P_0 = \phi_2 = 2702.2$ and the equivalent $T_0 = \frac{25}{36} \phi_3^2 = 3.038$.

The final shock Mach number $M_{S_1} (= 5.14)$ is obtained by a further interpolation from Table I.

This procedure was repeated for a range of values of p_6 and for various values of P_0 and the results are displayed as Fig. 6. A comparison of Fig. 6 with Fig. 4 demonstrates that this second type of double-diaphragm shock tube is slightly less efficient than the reflected shock type; for example, when $P_0 = 10^4$, $p_{6,1} = 10^3$, the former type gives $M_{S_1} = 5.14$, the latter $M_{S_1} = 5.22$, compared with the single-diaphragm value $M_{S_1} = 3.85$.

6. Multiple-Diaphragm Shock Tubes

Inspection of Figs. 4 and 6 shows that for maximum gain of shock Mach number M_S the intermediate pressure must be approximately the geometric mean of the pressures p_m and p_n where $p_{m,n} = P_0$. Hence a multiple-diaphragm shock tube may be postulated with n diaphragms and an overall pressure ratio P_0 such that

$$P_0 = p_I^n \dots (6.1)$$

where p_I is the individual pressure ratio across each diaphragm of a multiple-diaphragm shock tube.

6.1 Direct Calculations of Performance from Tables I and III

Consideration is next given to the reflected shock type of multiple-diaphragm shock tube; the flow pattern which occurs in this typical shock tube is shown in Fig. 7. The computation of the final shock Mach number M_{S_1} is made in discrete steps; and each step is identical with the procedure outlined in Section 4.2. Fig. 8 presents curves of shock Mach number M_{S_1} against number of diaphragms n for various overall pressure ratios P_0 . It may be noted that these curves tend to asymptotic values as n is increased: the gain of shock Mach number is most marked for high P_0 values. In the next section a generalised analysis is presented which derives approximate asymptotes for the $(M_{S_1} - n)$ curves.

6.2 General Analysis

Consider a diaphragm separating pressures p_m and p_n and let a shock M_{sm} strike the diaphragm and be reflected. Subsequently, the diaphragm may be ruptured and so produces a further shock M_{sn} (as in Fig. 3, where $m = 6$ and $n = 1$). From equations (3.1), (4.1) and (4.2) the following general expression relating M_{sn} , M_{sm} and p_{mn} may be derived.

$$p_{mn} = \frac{\left[\frac{2\gamma_n}{\gamma_n+1} M_{sn}^2 - \frac{\gamma_n-1}{\gamma_n+1} \right] \left[\frac{(\gamma_m-1) M_{sm}^2 + 2}{(3\gamma_m-1) M_{sm}^2 - 2(\gamma_m-1)} \right] \left[\frac{2\gamma_m}{\gamma_m+1} M_{sm}^2 - \frac{\gamma_m-1}{\gamma_m+1} \right]^{-1}}{\left[1 - \frac{\gamma_m-1}{\gamma_n+1} \right] (\gamma_m+1) \left(\frac{M_{sm}}{M_{sn}} \right) \frac{(M_{sn}^2 - 1)}{\sqrt{\{ (3\gamma_m-1) M_{sm}^2 - 2(\gamma_m-1) \} \{ 2(\gamma_m-1) M_{sm}^2 - (3-\gamma_m) \}}} } \right] \frac{2\gamma_m}{\gamma_m-1}} \dots(6.2)$$

Now consider a shock tube having a very large number of diaphragms; that is, suppose

$$p_m = p_n + dp_n$$

and $M_{sn} = M_{sm} + dM_{sm}$ (6.3)

Equation (6.2) still holds but must be put in the form

$$p_{mn} = 1 + \frac{dp_n}{p_n} = \text{function of} \left(1 + \frac{dM_{sn}}{M_{sm}} \right).$$

In order to shorten the tedious reduction of (6.2) it has been assumed that $\gamma_m = \gamma_n = 1.4$.

Then

$$p_{mn} = \frac{\left[\frac{7M_{sn}^2 - 1}{7M_{sn}^2 - 1} \right] \left[\frac{M_{sn}^2 + 5}{8M_{sm}^2 - 2} \right]}{\left[1 - \frac{1}{2} \frac{M_{sm}}{M_{sn}} \frac{(M_{sn}^2 - 1)}{\sqrt{(4M_{sm}^2 - 1)(M_{sm}^2 + 2)}}} \right]^7} \dots(6.4)$$

and, in differential form, after considerable reduction (6.4) becomes

$$1 + \frac{dp_n}{p_n} = f_1(M_{sn}) \{ 1 + f_2(M_{sm}) dM_{sm} \} \dots(6.5)$$

where $f_1(M_{sn}) = \left[\frac{M_{sn}^2 + 5}{8M_{sm}^2 - 2} \right] \left[1 - \frac{1}{2} \frac{(M_{sn}^2 - 1)}{\sqrt{(4M_{sm}^2 - 1)(M_{sm}^2 + 2)}}} \right]^{-7}$ (6.6)

and/

$$\text{and } f_2(M_{S_{in}}) = \left\{ \frac{14M_{S_{in}}}{7M_{S_{in}}^2 - 1} + \frac{7(M_{S_{in}}^2 - 1)}{2M_{S_{in}} \sqrt{(4M_{S_{in}}^2 - 1)(M_{S_{in}}^2 + 2) - M_{S_{in}}(M_{S_{in}}^2 - 1)}} \right\} \dots(6.7)$$

Examination of the functions $f_1(M_S)$ and $f_2(M_S)$ led to their replacement by

$$f_1(M_S) \cong 1.0 \dots(6.8)$$

$$f_2(M_S) \cong \frac{14}{3M_S}$$

Calculated values of the functions are given in Table V and the functions and their approximations are compared graphically in Fig. 9.

Then, approximately,

$$1 - \frac{d_p}{p} = 1 \left\{ 1 + \frac{14}{3M_S} dM_S \right\}$$

so that
$$\frac{d_p}{p} = \frac{14}{3} \frac{dM_S}{M_S} \dots(6.9)$$

On integration, (6.9) becomes

$$M_{S_{max}} = P_0^{\frac{3}{14}} \dots(6.10)$$

(Note it has been assumed that M_S increases as p decreases),

and, also,
$$\left(\frac{M_{S_1}}{M_{S_n}} \right)^{\frac{1}{3}} = \frac{p_1}{p_n} = P_0^{\frac{1}{14}} \dots(6.11)$$

if it is postulated that there is an equal pressure ratio across each diaphragm of the multiple-diaphragm shock tube.

Equation (6.10) shows that, irrespective of the number of diaphragms used in a multiple-diaphragm shock tube, the maximum possible shock Mach number is a function only of the overall pressure ratio across the ends of a shock tube. Calculated values of $M_{S_{max}}$ for various P_0 are:-

P_0	10	10^2	10^3	10^4	10^5
$M_{S_{max}}$	1.64	2.68	4.39	7.20	11.79

These maximum values of M_S are plotted on Fig. 8 and the agreement with values calculated from the general Tables I and III is very satisfactory.

Before discussing the general results of the preceding sections it is convenient to consider shock tubes having a discontinuous change of cross-section at a diaphragm station or at any other position along the tube, and to calculate the improvements in shock Mach number attainable by these methods.

7. Shock Tubes with Area Discontinuities

Modifications to shock tube geometry have been considered in several reports^{2,5,6} and the general results are derived herewith for completeness.

7.1 Area Discontinuity at the Diaphragm Station

To make the most economical use of the initial pressure ratio across the diaphragm it is desirable to use a shock tube which has a steady flow transition section from the chamber to the channel.

The most efficient conversion of heat energy to kinetic energy is

required and it is known that the quantity $\frac{du}{da}$ (which is a measure of this energy conversion) is, for Mach numbers less than unity, greater for a steady flow expansion than for an unsteady flow expansion. In mathematical terms, for a steady flow expansion the energy equation is

$$\frac{2}{\gamma - 1} a^2 + u^2 = \text{constant}$$

so that
$$\left(\frac{du}{da}\right)_{\text{steady}} = -\frac{2}{\gamma - 1} \frac{1}{M} \dots(7.1)$$

For an unsteady flow expansion

$$\frac{2}{\gamma - 1} a + u = \text{constant}$$

and hence
$$\left(\frac{du}{da}\right)_{\text{unsteady}} = -\frac{2}{\gamma - 1} \dots(7.2)$$

Hence it is desirable to use a shock tube where a steady flow expansion accelerates the "driver gas" (originally in the chamber) to a Mach number of unity and then an unsteady flow expansion further accelerates the gas to the velocity necessary to satisfy the velocity boundary condition at the contact surface.

Consider the shock tube flow pattern given in Fig. 10(a). There is steady flow in the region (5) to (4)* and unsteady flow in the other regions. If the overall pressure ratio P_0 is such that $M_3 > 1$, the steady flow expansion from region (5) to region (4) cannot continue after $M_4 = 1$ at the diaphragm station; the tube is effectively "choked" and a contoured throat would be necessary to accelerate the steady flow to $M_3 (>1)$. Since no such throat is present, a second rarefaction wave R_2 must be formed which accelerates the flow from $M_4 = 1$ at the diaphragm station to M_3 behind the contact surface. If $M_3 < 1$, the unsteady expansion wave R_2 is absent; furthermore if the area ratio $A_{s1} \rightarrow \infty$, $M_3 \rightarrow 0$ and the first rarefaction wave R_1 disappears.

Now, for a given shock Mach number M_{S1} , let us compare a non-uniform shock tube with the corresponding uniform shock tube. Consider Figs. 10(b) and 10(c) where $A_{s1} = \infty$ and unity respectively.

For/

*The smooth change of area shown in Fig. 10(a) would become a sharp discontinuous change in practice - this does not affect the subsequent analysis.

For any Mach number M_3 behind the contact surface the diagrams of the flow in the channels of the two shock tubes are identical. Hence any advantage due to the use of a non-uniform tube arises from the flow in the chamber section.

Now, for the steady flow expansion, Fig. 10(b), since $M_6 = 0$, it follows that

$$(p_{s4})_{A_{s1}=\infty} = \left[1 + \frac{\gamma - 1}{2} M_4^2 \right]^{\frac{\gamma}{\gamma-1}} \dots (7.3)$$

and

$$(T_{s4})_{A_{s1}=\infty} = 1 + \frac{\gamma - 1}{2} M_4^2. \dots (7.4)$$

Further, for the unsteady flow expansion, Fig. 10(c)

$$(p_{s4})_{A_{s1}=1} = \left[\left(1 + \frac{\gamma - 1}{2} M_4^2 \right)^2 \right]^{\frac{\gamma}{\gamma-1}} \dots (7.5)$$

and

$$(T_{s4})_{A_{s1}=1} = \left(1 + \frac{\gamma - 1}{2} M_4^2 \right)^2. \dots (7.6)$$

Note that, since T_4 is independent of A_{s1} , it follows from (7.4) and (7.6) that $(T_s)_{A_{s1}=\infty} \neq (T_s)_{A_{s1}=1}$.

Now, since $M_4 < 1$ and since p_{41} is independent of A_{s1} , a gain factor $G(\geq 1)$ may be defined as

$$G = \frac{(p_{s1})_{A_{s1}=1}}{(p_{s1})_{A_{s1}=\infty}} = \frac{\left[\left(1 + \frac{\gamma - 1}{2} M_4^2 \right)^2 \right]^{\frac{\gamma}{\gamma-1}}}{1 + \frac{\gamma - 1}{2} M_4^2} \dots (7.7)$$

When $M_4 = 1$, G has a maximum value - equal to $\left(\frac{\gamma + 1}{2} \right)^{\frac{\gamma}{\gamma-1}}$ -

and if $\gamma = 1.4$

$$G_{\max} = (1.2)^{2.5} = 1.893. \dots (7.8)$$

Thus, to produce a given shock Mach number M_{s1} the ratio p_{s1} for the non-uniform shock tube is smaller than that for a uniform shock tube: or, in other words, for the same overall pressure ratio P_0 the non-uniform shock tube produces a stronger shock than the uniform shock tube. If the general case (Fig. 10(a)) where A_{s1} is finite and greater than unity is reconsidered, a general expression for the gain factor G is obtained in terms of M_5 and M_4 where M_5 is related to A_{s1} by the steady flow expansion equation

$$A_{s1} = \frac{M_2}{M_5} \left[\frac{1 + \frac{1}{2}(\gamma - 1) M_5^2}{1 + \frac{1}{2}(\gamma - 1) M_4^2} \right]^{\frac{\gamma+1}{2(\gamma-1)}} \dots(7.9)$$

The effects of the rarefaction wave R_1 may be incorporated in the preceding analysis by noting that

$$P_{s5} = \left[1 + \frac{\gamma - 1}{2} M_5^2 \right]^{\frac{\gamma}{\gamma-1}} \dots(7.10)$$

and hence it follows that

$$G = \left[\frac{1 + \frac{1}{2}(\gamma - 1) M_5^2}{1 + \frac{1}{2}(\gamma - 1) M_4^2} \left\{ \frac{1 + \frac{1}{2}(\gamma - 1) M_4^2}{1 + \frac{1}{2}(\gamma - 1) M_5^2} \right\}^2 \right]^{\frac{\gamma}{\gamma-1}} \dots(7.11)$$

To sum up, if $A_{s1} \geq 1$ then $G \geq 1$ for a given M_5 ; further if $M_3 \geq 1$ G is a function of A_{s1} but independent of P_{s1} , but, if $M_3 < 1$, G is a function of P_{s1} and A_{s1} .

In the present context the maximum advantage to be obtained from the use of non-uniform shock tubes is required; it is therefore assumed that $M_3 > 1$ and hence $M_2 = 1$. If $\gamma = 1.4$, the equations (7.9) and (7.11) become

$$A_{s1} = \frac{1}{M_5} \left[\frac{5 + M_5^2}{6} \right]^3 \dots(7.12)$$

and

$$G = \left[6 \left\{ \frac{5 + M_5^2}{(5 + M_5^2)^2} \right\} \right]^{3.5} \dots(7.13)$$

Equation (7.12) is plotted as Fig. 11(a), equation (7.13) is plotted as Fig. 11(b) and Fig. 11(c) is a cross plot - from the previous two figures - giving the variation of G with A_{s1} .

Finally, the performance of this type of shock tube may be computed. Given A_{s1} , the gain factor G is known from the curve of Fig. 11(c); this gain is achieved provided $M_3 \geq 1$. The problem then reduces to an equivalent uniform shock tube where the overall pressure ratio is GP_0 and the overall temperature ratio is

$\frac{\gamma-1}{\gamma} T_0^*$ Hence the maximum possible gain of M_{s1} for a given P_0 and T_0^* will be obtained when M_{s1} is calculated from equation (3.3) in the form

$$1.893 P_0 = \left\{ \frac{7M_{s1}^2 - 1}{6} \right\} \left\{ 1 - \frac{(1.2 T_0^*)^{-\frac{1}{2}}}{6} \left\{ \frac{M_{s1}^2 - 1}{M_{s1}} \right\} \right\}^{-7} \dots(7.14)$$

A/

*From (7.3) to (7.7) inclusive, $G_{max} = 1.893$, and

$$G_{max}^{\frac{\gamma-1}{\gamma}} = 1.2$$

A curve of M_{S_1} for a non-uniform shock tube was calculated from (7.14) for various P_0 and $T_0 = 1$. This curve is plotted on Fig. 12 for comparison with the double and multiple-diaphragm types of shock tube.

7.2. Area Discontinuity at a Point along the Shock Tube

Let us consider the shock tube illustrated in Fig. 10(d). Suppose the area ratio A_{s_1} is very large and let the shock M_{S_6} hit the area discontinuity. This shock will be reflected, leaving region (4) at rest; subsequently a steady expansion occurs and the problem is exactly the same as that treated in Section 7.1 above - the gain in shock Mach number is thus related to the Gain Factor G. If the area ratio A_{s_1} is not infinite the reflected shock is not so strong, $M_4 \neq 0$ and the possible gain is therefore reduced.⁶

It may be noted that the delay required before the breakage of the second diaphragm of the reflected-shock type of double-diaphragm shock tube (see Section 4) may be reduced to zero (that is, breakage of diaphragm by shock impact) if there is a considerable area decrease at the second diaphragm station. In this manner the analysis of Section 4 may be applied to a multiple-diaphragm shock tube if there is a large area decrease at a diaphragm which is broken by shock impact, but without such area decrease the analysis of Section 5 must be used.

8. Special Types of Shock Tube

8.1. The Constant Mach Number Shock Tube

In Section 3.2 consideration was given to a special type of simple shock tube in which the Mach number of the flow between the shock and the contact surface is the same as the Mach number of the flow between the contact surface and the rarefaction wave. Such a shock tube possesses the important advantage that the available testing time is increased by a factor of about 7 for the very strong shock wave case; in particular, this improvement in testing time would ease considerably the formidable instrumentation problems encountered with hypersonic shock tubes.

It has been noted that to produce strong shock waves in a simple shock tube, the initial temperature ratio T_0 must be considerably larger than the values normally employed. Since the multiple-diaphragm shock tube effectively exchanges a decrease of pressure ratio in favour of an increase in temperature ratio, the variables P_0 and T_0 across the final diaphragm may be adjusted to give a final 'constant Mach number' shock tube flow. Consider the reflected shock type of multiple-diaphragm shock tube shown in Fig. 7 and let shock M_{S_6} be reflected from diaphragm D_3 in the usual manner. It may be calculated that if the pressure ratio p_{s_1} is about 1.0 to 1.5, depending on M_{S_6} , conditions in the final channel will satisfy the 'constant Mach number' case; that is $M_2 \approx M_3$. It is therefore suggested that only a minor mismatch between M_2 and M_3 would occur if $p_{s_1} = 1.0$. Hence, in practice the required final shock Mach number M_{S_6} would be produced and then subsequently the shock tube flow would be converted to the 'constant Mach number' condition by the addition of a further diaphragm with zero pressure difference across it.

8.2 The Performance of Diaphragms having Zero Pressure Difference Across them

Consider a shock wave of shock Mach number M_{S_1} which is reflected from a diaphragm having zero pressure difference across it. Subsequently let the diaphragm be ruptured and let the resultant shock Mach number be M_{S_2} .

From/

From the general formula (6.4) with $dp = 0$ and $y = 1.4$, it follows that

$$\left[\frac{7M_{S_1}^2 - 1}{7M_{S_2}^2 - 1} \right] \left[\frac{8M_{S_1}^2 - 2}{M_{S_1}^2 + 5} \right] = \left[1 - \frac{1}{2} \frac{M_{S_1}}{M_{S_2}} \frac{(M_{S_2}^2 - 1)}{\sqrt{(4M_{S_1}^2 - 1)(M_{S_1}^2 + 2)}} \right]^{-7} \quad \dots(8.1)$$

Let $M_{S_1} \gg 1$ and $M_{S_2} = M_{S_1} + dM_{S_1} \gg 1$ so that

$$\frac{M_{S_2}^2}{8M_{S_1}^2} = \left\{ 1 - \frac{M_{S_2}}{4M_{S_1}} \right\}^7 \quad \dots(8.2)$$

Now suppose $M_{S_2} = kM_{S_1}$, ... (8.3)

then (8.2) yields $\frac{k^2}{8} = \left(1 - \frac{k}{4} \right)^7$... (8.4)

which is satisfied by one real value of k , that is, $k = 1.01525$

$$k = 1.01525. \quad \dots(8.5)$$

Thus, in the limit as $M_S \gg 1$, the gain of shock Mach number by this method is 1.5%. Now consider equation (6.5), with $dp = 0$, namely:-

$$1 = f_1(M_S) \{ 1 + f_2(M_S) dM_S \}, \quad \dots(8.6)$$

and refer to Table V where $f_1(M_S)$ and $f_2(M_S)$ are tabulated.

Note that if $M_S < 2.077$, dM_S is negative; if $M_S = 2.077$, $dM_S = 0$ and if $M_S > 2.077$, dM_S is positive.

Alternatively the increments in shock Mach number dM_S may be calculated directly from Tables III and I: these results are given in Table VII. These calculations show that

- if $M_S < 2.67$, dM_S is negative
- if $M_S = 2.67$, dM_S is zero
- and if $M_S > 2.67$, dM_S is positive.

The inconsistency between these two methods is presumably due to the assumption that dM_S is infinitesimal in the theory but finite in the tables.

The results for multiple-diaphragm shock tubes may be summarised as follows. Let the number of diaphragms n be very large so that the pressure difference dp across each diaphragm is small. If $dp \neq 0$, the maximum attainable shock Mach number M_S increases as n increases to a limit which is a function of the overall pressure ratio across the extreme ends of the shock tube. If a shock of Mach number greater than 2.67 is allowed to strike a series of diaphragms each with zero pressure difference across it, then the maximum attainable shock Mach number increases without limit. On the other hand, if the initial shock Mach number is less than 2.67, shock decay will take place.

8.3 Duration of Flow in Multiple Diaphragm Shock Tubes

The available flow durations may be calculated by standard methods¹; the multiple diaphragms may be conveniently grouped near the high pressure end of the shock tube since the flow duration merely depends upon L , M_{S_1} and M_2 (see Fig. 7) according to the equation

$$\frac{\tau_L}{L} = \frac{1}{a_2 M_2} - \frac{1}{a_1 M_{S_1}} \quad \dots(8.7)$$

9. Discussion and Conclusions

9.1 Resumé of Results

The maximum possible gains in shock Mach number M_s over that obtainable using a simple shock tube with the same initial conditions are illustrated in Fig. 12 and Table VI for each type of modified shock tube discussed in this paper.

It is clear that shock tubes with area discontinuities are not of much practical use when the overall pressure ratio P_0 exceeds 10^3 (say); the increase of shock Mach number thus obtained is small whilst structural costs would become prohibitive even for moderate area ratios. The double-diaphragm technique appears to be extremely simple and offers a considerable increase of shock Mach number; in practice the unsteady expansion type would probably be used since it does not require the electronic delay equipment needed for the reflected shock technique. In view of the very large gains of shock Mach number indicated by the theory of multiple diaphragm shock tubes with high overall pressure ratios, there is a need for experimental investigation of these types of shock tubes.

9.2 The Performance Calculations

The Tables and Figures in this report have been calculated from perfect gas theory. This implies that, in order to avoid the effects of dissociation (above 3000°K) and ionisation (above 4500°K), the calculations of P_0 from equation (3.3) must be restricted to $M_s \dagger 8.0$ and $T_0 \dagger 15$ assuming $T_1 \doteq 238^\circ\text{K}$ initially. Thus Table I does not involve appreciable errors due to gaseous imperfections.

Unfortunately it is not possible to apply the general results of the Tables to cases where $\gamma \neq 1.4$, but the calculation of the performance of shock tubes using any other possible gas combination or combinations follows from the general formulae which have been derived above.

9.3 Conclusions

From the performance calculations for multiple-diaphragm shock tubes presented herein, it is concluded that an experimental investigation of these shock tubes would be valuable. Attention is drawn to the 'constant Mach number' mode of operation of shock tubes: this feature of multiple-diaphragm shock tubes may be a useful addition to the hypersonic shock tube technique.

Acknowledgements

Miss C. M. Tracy and Mr. P. J. Peggs performed the computations and Dr. G. E. Gadd and Mr. E. W. E. Rogers offered helpful suggestions.

References

<u>No.</u>	<u>Author(s)</u>	<u>Title, etc.</u>
1	B. D. Henshall	Some Notes on the Flow Durations occurring in Hypersonic Shock Tubes. A.R.C.17,608 - F.M.2243 - T.P.461. 11th August, 1955.
2	J. Lukasiewicz	Shock Tube Theory and Applications. N.A.E., Canada, Report 15, 1952. A.R.C.15,653 - T.P.385 - F.M.1963. 18th February, 1953.
3	B. D. Henshall	On Some Aspects of the use of Shock Tubes in Aerodynamic Research. University of Bristol, Dept. of Aeronautical Engineering Report No.P.4. Communicated by Prof. A. R. Collar. A.R.C.17407 - T.P.449. 24th February, 1955. and Corrigendum, 13th July, 1955.
4	H. Bernstein	A Double-Diaphragm Shock Tube to produce Transient High Mach Number Flows. J.Ae.Sci., Vol.20, No.11, pp.790-791, November, 1953. A.R.C.17549 - F.M.2225. 7th April, 1955.
5	E. L. Resler, S. C. Lin and A. Kantrowitz	The Production of High Temperature Gases in Shock Tubes. J. Appld. Phys., Vol.23, No.12, p.1390, December, 1952.
6	O. Laporte	On the Interaction of a Shock with a Constriction. Los Alamos Scientific Laboratory Report LA-1740, January, 1955.

APPENDIX

APPENDIX

Interpolation from Table I to Determine M_s

Given the initial overall pressure ratio P_0 and temperature ratio T_0 across a diaphragm, the shock Mach number M_s which is produced when the diaphragm is ruptured may be calculated as follows.

As an example of the method of interpolation, consider the case

$$P_0 = 42,513, \quad T_0 = 2.496.$$

From Table I, from the columns of T_0 ,

<u>$T_0 = 2$</u>		<u>$T_0 = 3$</u>	
$M_s = 5.5$	$P_0 = 34,603$	$M_s = 6.5$	$P_0 = 36,224$
$M_s = 5.6$	$P_0 = 45,513$	$M_s = 6.6$	$P_0 = 44,690$
Hence $M_s = 5.572$	$P_0 = 42,513$	Hence $M_s = 6.576$	$P_0 = 42,513.$
Then	$T_0 = 2.0$	$M_s = 5.572$	
	$T_0 = 3.0$	$M_s = 6.576.$	
Hence and	$T_0 = 2.496$ $P_0 = 42,513$	} gives $M_s = 6.070.$	

This method of successive linear interpolation was checked and found accurate to 1% for the intervals given in Table I.

TABLE I/

TABLE I. [Equation (3.3)]

Values of P_0 for Independent Ranges of I_0 and T_0

I_0 M_S	1	2	3	4	5	6	7
1.0	1.0	1.0	1.0	1.0	1.0	1.0	1.0
1.1	1.5612	1.4599	1.4175	1.3928	1.3763	1.3644	1.3552
1.2	2.3532	2.0616	1.9460	1.8806	1.8295	1.8060	1.7823
1.3	3.4516	2.8368	2.6049	2.4776	2.3944	2.3349	2.2902
1.4	4.9580	3.8236	3.4184	3.2003	3.0605	2.9620	2.8880
1.5	7.0020	5.0684	4.4131	4.0681	3.8512	3.6990	3.5858
1.6	9.7571	6.6270	5.6204	5.1033	4.7823	4.5595	4.3950
1.7	13.453	8.5656	7.0763	6.3295	5.8724	5.5584	5.3277
1.8	18.389	10.966	8.8234	7.7760	7.1416	6.7120	6.3982
1.9	24.966	14.767	10.912	9.4737	8.6156	8.0400	7.6224
2.0	33.713	17.562	13.400	11.459	10.319	9.5601	9.0154
2.1	45.342	22.021	16.354	13.774	12.283	11.299	10.595
2.2	60.797	27.470	19.852	16.466	14.538	13.278	12.385
2.3	81.360	34.128	23.982	19.590	17.123	15.527	14.406
2.4	108.77	42.248	28.857	23.210	20.080	18.079	16.680
2.5	145.35	52.137	34.594	27.393	23.458	20.966	19.236
2.6	194.32	64.183	41.348	32.213	27.307	24.229	22.109
2.7	260.11	78.851	49.282	37.780	31.688	27.908	25.323
2.8	348.84	96.700	58.596	44.180	36.670	32.052	28.924
2.9	468.99	118.44	69.527	51.550	42.328	36.724	32.949
3.0	632.60	144.94	82.357	60.010	48.744	41.965	37.440
3.1	856.54	177.21	97.525	69.739	56.020	47.858	42.443
3.2	1165.3	216.62	115.01	80.896	64.253	54.468	48.026
3.3	1593.6	264.72	135.67	93.706	73.582	61.876	54.241
3.4	2192.7	323.60	159.90	108.41	84.144	70.179	61.144
3.5	3041.5	396.03	188.44	125.31	96.112	79.504	68.846
3.6	4239.6	484.16	221.70	144.59	109.56	89.902	77.374
3.7	5970.1	592.96	260.84	166.77	124.81	101.55	86.848

TABLE I (contd.)

TABLE I (contd.)

T_0 T_s	1	2	3	4	5	6	7
3.8	8483.2	727.10	306.82	192.20	142.07	114.58	97.383
3.9	12198	892.62	360.92	221.36	161.55	129.15	109.06
4.0	1774.0	1097.5	424.52	254.85	183.55	145.44	122.03
4.1	26145	1351.8	499.12	293.26	208.42	163.66	136.38
4.2	39122	1668.4	587.76	337.38	236.55	184.02	152.34
4.3	59519	2063.8	692.05	380.07	268.29	206.77	169.97
4.4	92275	2559.4	815.24	446.30	304.20	232.23	189.58
4.5	141622	3182.6	961.05	513.30	344.78	260.63	211.26
4.6		3968.7	1133.8	590.45	390.76	292.45	235.34
4.7		4967.0	1338.7	679.18	442.73	327.99	261.99
4.8		6235.9	1582.5	781.53	501.46	367.70	291.53
4.9		7859.2	1872.9	899.68	568.04	412.10	324.23
5.0		9947.8	2219.4	1036.0	643.53	461.86	360.57
5.1		12648	2633.8	1193.5	729.04	517.45	400.85
5.2		16158	3130.2	1375.9	826.03	579.74	445.43
5.3		20745	3726.4	1587.2	936.03	649.46	495.00
5.4		26789	4444.3	1832.1	1061.2	727.52	549.85
5.5		34803	5309.7	2116.3	1203.1	815.03	610.77
5.6		45513	6357.7	2446.9	1364.8	913.21	678.52
5.7		59924	7628.6	2832.4	1548.6	1023.4	753.53
5.8		79512	9175.8	3281.3	1758.2	1146.6	836.86
5.9		106379	11065	3806.4	1997.3	1285.7	929.60
6.0		143599	13378	4420.1	2270.1	1441.7	1032.5
6.1			16225	5138.9	2581.7	1616.9	1147.1
6.2			19730	5984.0	2938.7	1814.3	1274.5
6.3			24073	6977.9	3346.5	2036.4	1416.3
6.4			29475	8148.4	3814.5	2286.6	1574.2
6.5			36224	9530.4	4352.1	2747.0	1750.1
6.6			44690	11169	4969.6	2887.7	1946.2
6.7			55358	13110	5680.2	3309.2	2165.1

TABLE I (contd.)//

TABLE I (contd.)

$\begin{matrix} T_0 \\ M_S \end{matrix}$	1	2	3	4	5	6	7
6.8			68864	15418	6500.0	3654.9	2409.5
6.9			86083	18173	7444.4	4115.7	2681.9
7.0			108137	21465	8537.6	4637.8	2986.9
7.1				25409	9801.5	5230.0	3327.8
7.2				30143	11270	5902.1	3709.7
7.3				35867	12974	6665.4	4137.1
7.4				42772	14956	7534.4	4615.8
7.5				51168	17266	8525.8	5153.8
7.6				61195	19908	9626.7	5741.0
7.7				73848	23128	10944	6435.9
7.8				89153	26835	12456	7199.4
7.9				108011	31192	14109	8059.8
8.0				131364	36327	16044	9029.0

TABLE I (contd.)//

TABLE I (contd.)

$M_S \backslash T_0$	8	9	10	11	12	13	14	15
1.0	1.0	1.0	1.0	1.0	1.0	1.0	1.0	1.0
1.1	1.3475	1.3415	1.3363	1.3318	1.3281	1.3247	1.3217	1.3190
1.2	1.7635	1.7479	1.7347	1.7226	1.7141	1.7056	1.6982	1.6916
1.3	2.2546	2.2258	2.2015	2.1810	2.1635	2.1479	2.1347	2.1217
1.4	2.8295	2.7824	2.7433	2.7098	2.6812	2.6562	2.6319	2.6146
1.5	3.4973	3.4259	3.3667	3.3167	3.2736	3.2364	3.2037	3.1744
1.6	4.2672	4.1647	4.0796	4.0079	3.9477	3.8946	3.8478	3.8071
1.7	5.1495	5.0079	4.8907	4.7931	4.7089	4.6366	4.5735	4.5171
1.8	6.1574	5.9666	5.8094	5.6779	5.5664	5.4704	5.3864	5.3114
1.9	7.3036	7.0512	6.9276	6.6733	6.5275	6.4025	6.2930	6.1964
2.0	8.6009	8.2745	8.0095	7.7892	7.6019	7.4419	7.3017	7.1791
2.1	10.066	9.6495	9.3118	9.0339	8.7967	8.5963	8.4208	8.2662
2.2	11.714	11.191	10.768	10.420	10.125	9.8739	9.6568	9.4657
2.3	13.568	12.915	12.391	11.959	11.596	11.288	11.021	10.787
2.4	15.643	14.838	14.194	13.664	13.222	12.846	12.521	12.236
2.5	17.963	16.980	16.194	15.552	15.018	14.562	14.169	13.828
2.6	20.553	19.360	18.410	17.638	16.993	16.446	15.976	15.566
2.7	23.442	21.999	20.860	19.933	19.164	18.511	17.953	17.468
2.8	26.655	24.926	23.567	22.461	21.546	20.776	20.113	19.541
2.9	30.227	28.166	26.549	25.238	24.160	23.250	22.473	21.799
3.0	34.192	31.748	29.828	28.288	27.018	25.951	25.024	24.252
3.1	38.593	35.697	33.446	31.632	30.148	28.902	27.837	26.923
3.2	43.466	40.061	37.415	35.294	33.563	32.113	30.880	29.818
3.3	48.862	44.861	41.770	39.307	37.289	35.609	34.186	32.963
3.4	54.823	50.156	46.549	43.685	41.355	39.416	37.774	36.364
3.5	61.441	55.994	51.800	48.487	45.791	43.559	41.670	40.051
3.6	68.708	62.375	57.526	53.700	50.608	48.041	45.876	44.029
3.7	76.762	69.405	63.815	59.408	55.851	52.916	50.442	48.333
3.8	85.644	77.138	70.696	65.634	61.555	58.198	55.379	52.966

TABLE I (contd.)

TABLE I (contd.)

T_0 M_S	8	9	10	11	12	13	14	15
3.9	95.433	85.622	78.195	72.408	67.745	63.926	60.722	57.996
4.0	106.25	94.927	86.414	79.787	74.480	70.123	66.502	63.414
4.1	118.14	105.12	95.389	87.819	81.780	76.847	72.726	69.248
4.2	131.28	116.32	105.18	96.573	89.715	84.113	79.474	75.540
4.3	143.58	128.59	115.87	106.08	98.305	91.974	86.733	82.307
4.4	161.64	142.04	127.52	116.42	107.62	100.47	94.582	89.596
4.5	179.18	156.76	140.29	127.66	117.72	109.66	103.03	97.458
4.6	198.47	172.89	154.15	139.87	128.67	119.61	112.14	104.89
4.7	219.71	190.56	169.30	153.15	140.50	130.33	121.96	114.97
4.8	241.93	209.91	185.80	167.59	153.32	141.90	132.55	124.72
4.9	268.89	231.05	203.79	183.22	167.22	154.42	143.94	135.22
5.0	297.21	254.27	223.40	200.21	182.25	167.90	156.20	146.50
5.1	328.45	279.64	244.78	218.70	198.51	182.46	169.42	158.59
5.2	362.81	307.41	268.05	238.72	216.12	198.18	183.62	171.60
5.3	400.58	337.83	293.40	260.45	235.15	215.13	198.92	185.54
5.4	442.26	371.13	321.06	284.06	255.75	233.42	215.38	200.54
5.5	488.17	407.61	351.15	309.67	278.01	253.12	233.07	216.62
5.6	538.75	447.53	383.99	337.43	302.11	274.39	252.13	233.85
5.7	594.38	491.27	419.76	367.62	328.18	297.30	272.57	252.40
5.8	655.76	539.13	458.73	400.32	356.28	322.04	294.62	272.25
5.9	723.40	591.49	501.17	435.88	386.81	348.67	318.27	293.53
6.0	797.92	648.97	547.40	474.40	419.70	377.41	343.73	316.41
6.1	880.07	711.86	597.84	516.20	455.36	408.35	371.07	340.96
6.2	970.77	780.80	652.79	561.64	493.86	441.74	400.50	367.23
6.3	1070.8	856.39	712.76	610.88	535.50	477.68	432.11	395.45
6.4	1181.2	939.27	778.09	664.40	580.55	516.52	466.12	425.69
6.5	1303.3	1030.2	849.39	722.49	629.28	588.34	502.73	458.08
6.6	1437.9	1129.8	927.10	785.54	681.99	603.36	541.95	492.86
6.7	1586.8	1239.2	1011.9	853.97	739.01	652.02	584.24	530.13
6.8	1751.4	1359.2	1104.6	928.39	800.70	704.40	629.65	570.14

TABLE I (contd.)

TABLE I (contd.)

T_0	8	9	10	11	12	13	14	15
6.9	1933.5	1941.1	1205.7	1009.2	867.30	760.90	678.41	613.00
7.0	2135.4	1635.9	1316.0	1097.1	939.64	821.86	730.98	659.01
7.1	2358.5	1795.2	1436.5	1192.5	1017.8	887.61	787.43	708.31
7.2	2605.9	1970.2	1568.2	1296.4	1102.3	958.55	848.17	761.23
7.3	2879.6	2162.5	1712.0	1409.2	1194.0	1034.9	913.39	818.04
7.4	3183.4	2374.1	1869.6	1531.7	1293.2	1117.5	983.57	878.92
7.5	3520.8	2607.2	2041.6	1665.0	1400.8	1206.6	1059.1	944.27
7.6	3884.2	2855.5	2223.1	1805.2	1512.6	1298.9	1137.2	1011.3
7.7	4311.8	3146.4	2435.8	1968.4	1643.3	1406.6	1228.1	1089.5
7.8	4775.4	3458.3	2661.0	2140.6	1780.2	1518.6	1322.0	1170.2
7.9	5290.4	3801.8	2931.2	2328.0	1928.2	1639.6	1423.4	1256.7
8.0	5863.8	4181.4	3178.7	2532.5	2088.8	1770.4	1532.6	1349.6

TABLE II/

TABLE II

Values of P_0 , T_0 and M_s for the
'Constant Mach Number' Shock Tube

M_s	P_0 Eqn. (3.10)	T_0 Eqn. (3.9)
1	1	1
2	15.443	2.400
3	55.584	4.332
4	122.92	6.952
5	216.42	10.294
6	333.60	14.370
7	475.00	19.171
8	635.67	24.716
9	827.48	30.984
10	1028.2	38.009
11	1258.2	45.810
12	1510.6	54.259

TABLE III/

TABLE III

The Reflection of a Shock Wave from a Rigid Wall

M_s	P_{4s} Eqn. (4.3)	T_{4s} Eqn. (4.4)	M_s	P_{4s} Eqn. (4.3)	T_{4s} Eqn. (4.4)
1.00	1.000	1.000	5.0	191.40	11.880
1.1	1.5397	1.1319	5.1	200.55	12.329
1.2	2.2371	1.2634	5.2	209.90	12.787
1.3	3.1082	1.3974	5.3	219.45	13.254
1.4	4.1669	1.5355	5.4	229.20	13.730
1.5	5.4250	1.6790	5.5	239.15	14.215
1.6	6.8932	1.8287	5.6	249.29	14.709
1.7	8.5791	1.9853	5.7	259.63	15.214
1.8	10.489	2.1492	5.8	270.16	15.722
1.9	12.629	2.3207	5.9	280.89	16.243
2.0	15.000	2.5000	6.0	291.81	16.772
2.1	17.607	2.6874	6.1	302.93	17.310
2.2	20.450	2.8830	6.2	314.24	17.856
2.3	23.530	3.0869	6.3	325.75	18.412
2.4	26.846	3.2992	6.4	337.44	18.977
2.5	30.400	3.5200	6.5	349.33	19.550
2.6	34.189	3.7493	6.6	361.42	20.133
2.7	38.211	3.9873	6.7	373.69	20.724
2.8	42.466	4.2339	6.8	386.16	21.324
2.9	46.952	4.5083	6.9	398.82	21.933
3.0	51.667	4.7531	7.0	411.67	22.551
3.1	56.609	5.0258	7.1	424.71	23.178
3.2	61.776	5.3072	7.2	437.94	23.814
3.3	67.165	5.5974	7.3	451.37	24.458
3.4	72.778	5.8963	7.4	464.98	25.112
3.5	78.609	6.2041	7.5	478.78	25.774
3.6	84.600	6.5206	7.6	492.78	26.445
3.7	90.923	6.8460	7.7	506.96	27.125
3.8	97.403	7.1802	7.8	521.33	27.814
3.9	104.10	7.5231	7.9	535.89	28.512
4.0	111.00	7.8750	8.0	550.65	29.219
4.1	118.11	8.2357	9	708.63	36.775
4.2	125.44	8.6052	10	885.40	45.220
4.3	132.97	8.9835	11	1082.3	54.617
4.4	140.71	9.3707	12	1295.3	64.776
4.5	148.65	9.7668	13	1528.5	75.887
4.6	156.79	10.172	14	1780.2	87.888
4.7	165.14	10.586	15	2089.7	102.68
4.8	173.69	11.008	16	2339.9	114.56
4.9	182.45	11.440	17	2647.8	129.22
5.0	191.40	11.880	18	2974.3	144.78
			19	3319.6	161.22
			20	3683.5	178.56

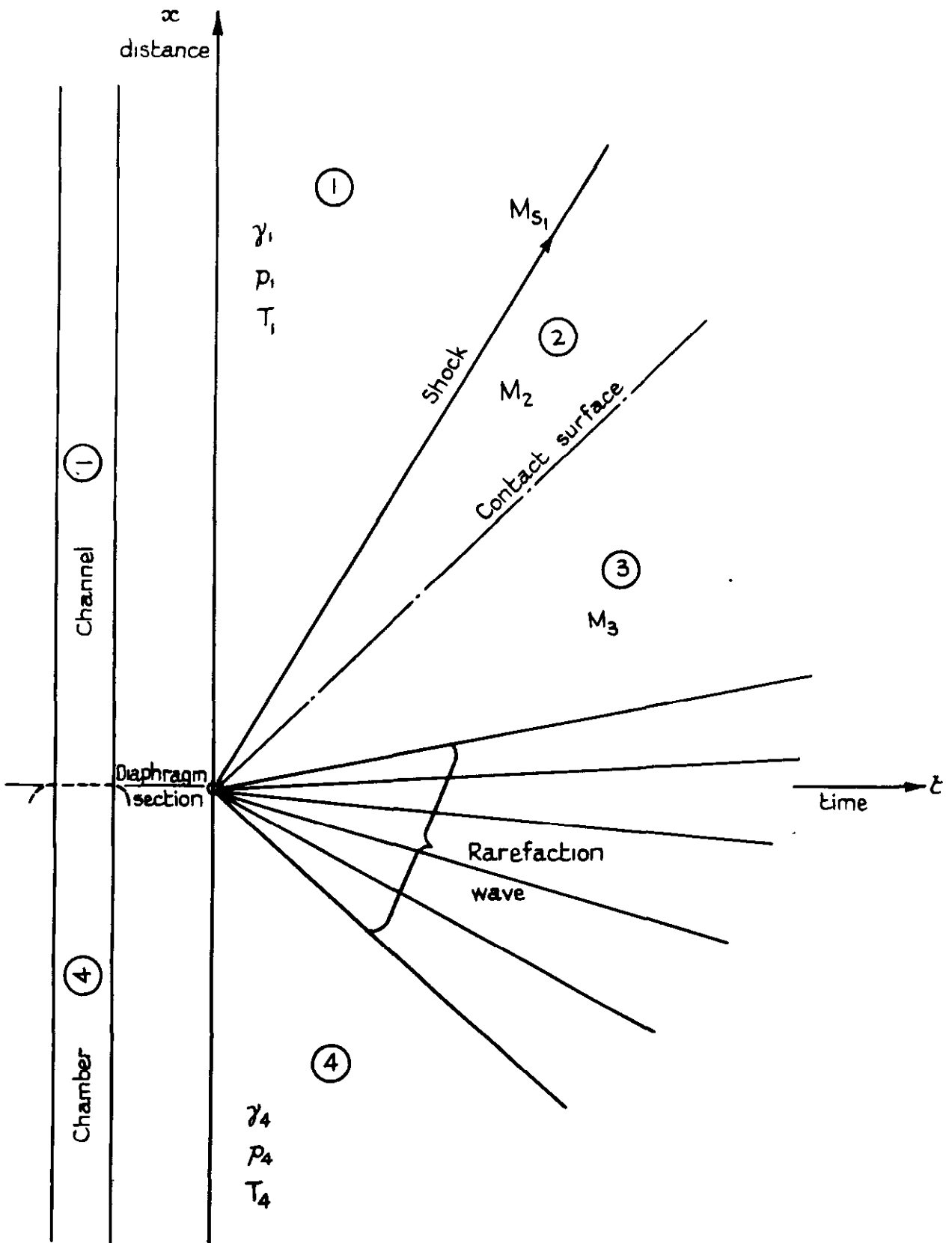
TABLE IV/

TABLE VII

Gain in M_s due to Reflection of a Shock from a
Diaphragm having Zero Pressure Difference across it.
 $T_o = 1$

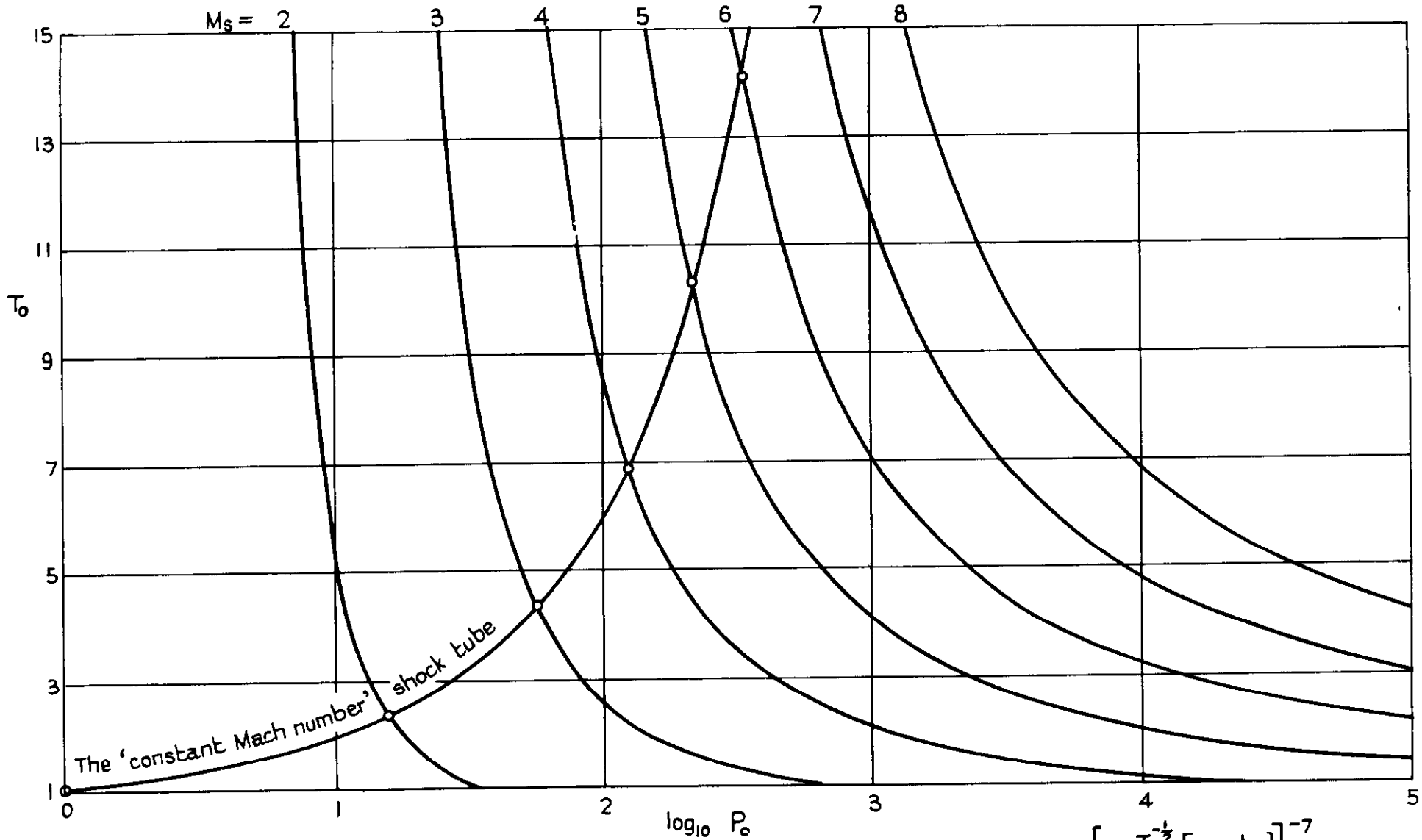
M_{s_1}	M_{s_2}	dM_s (Tables I and III)
1.0	1.000	0
1.5	1.491	-0.009
2.0	1.981	-0.019
2.5	2.497	-0.003
3.0	3.006	+0.006
3.5	3.515	+0.015
4.0	4.024	+0.024
4.5	4.533	+0.033
5.0	5.043	+0.043
5.5	5.557	+0.057
Very large	Very large	1.5% (Theory)

FIG. 1



A simple shock tube : Flow diagram

FIG. 2

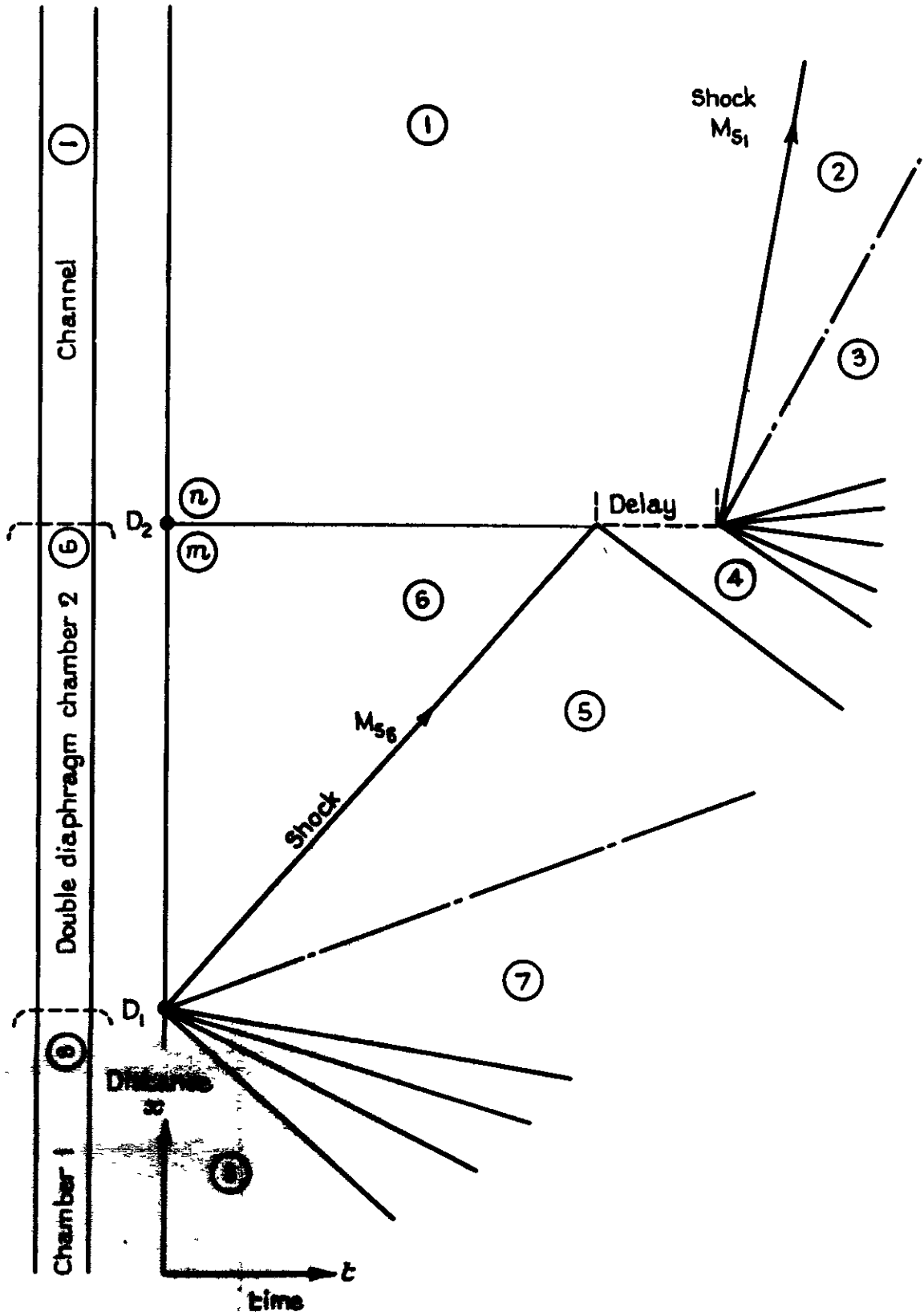


Results from Table I - Equation (3.3)

$$P_0 = \frac{1}{6} (7M_s^2 - 1) \left[1 - \frac{T_0^{-1/2}}{6} \left[M_s - \frac{1}{M_s} \right] \right]^{-7}$$

Variation of M_s with P_0 and T_0

Fig. 3.



Double - diaphragm shock tube - reflected shock type : flow diagram

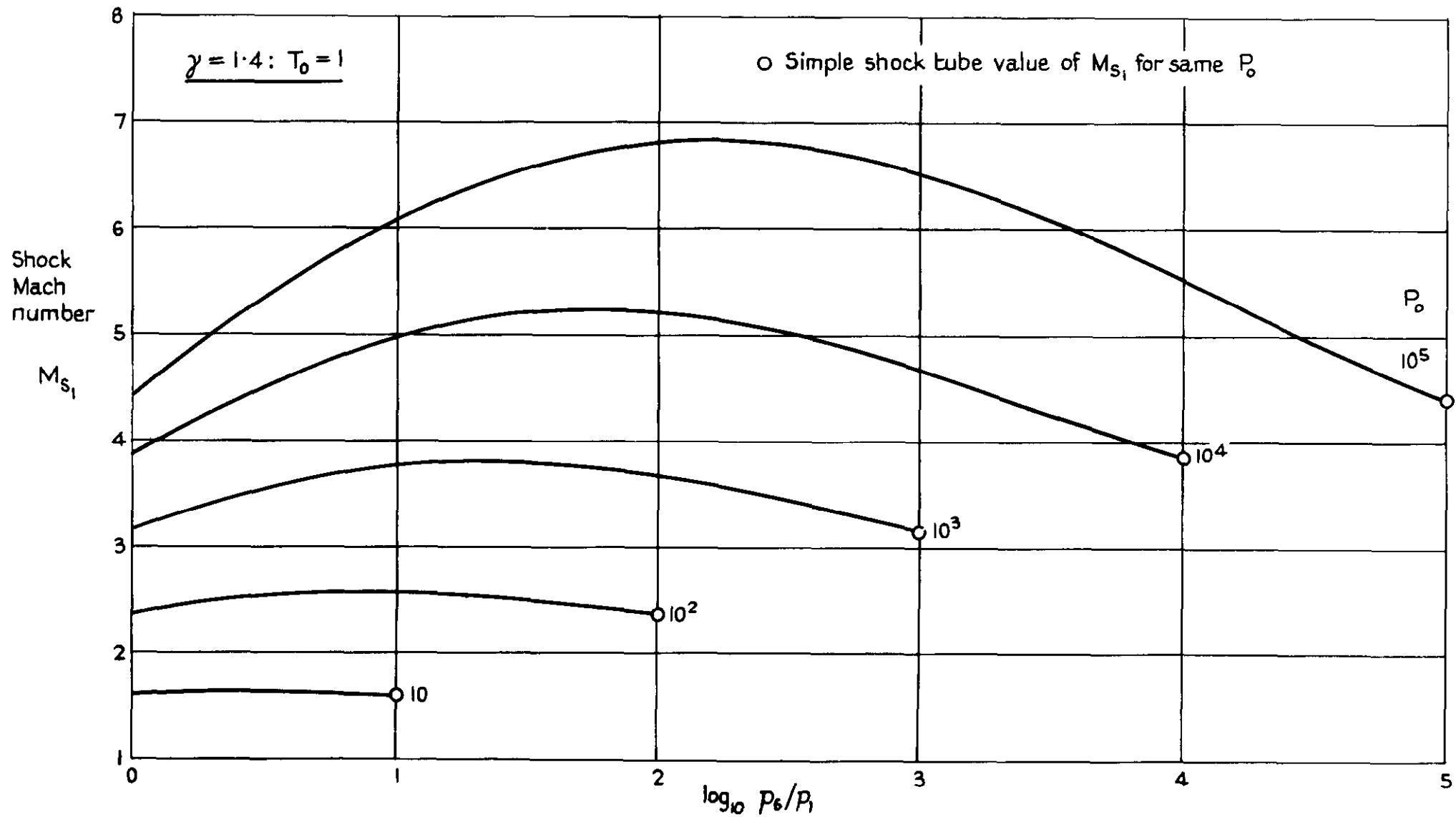
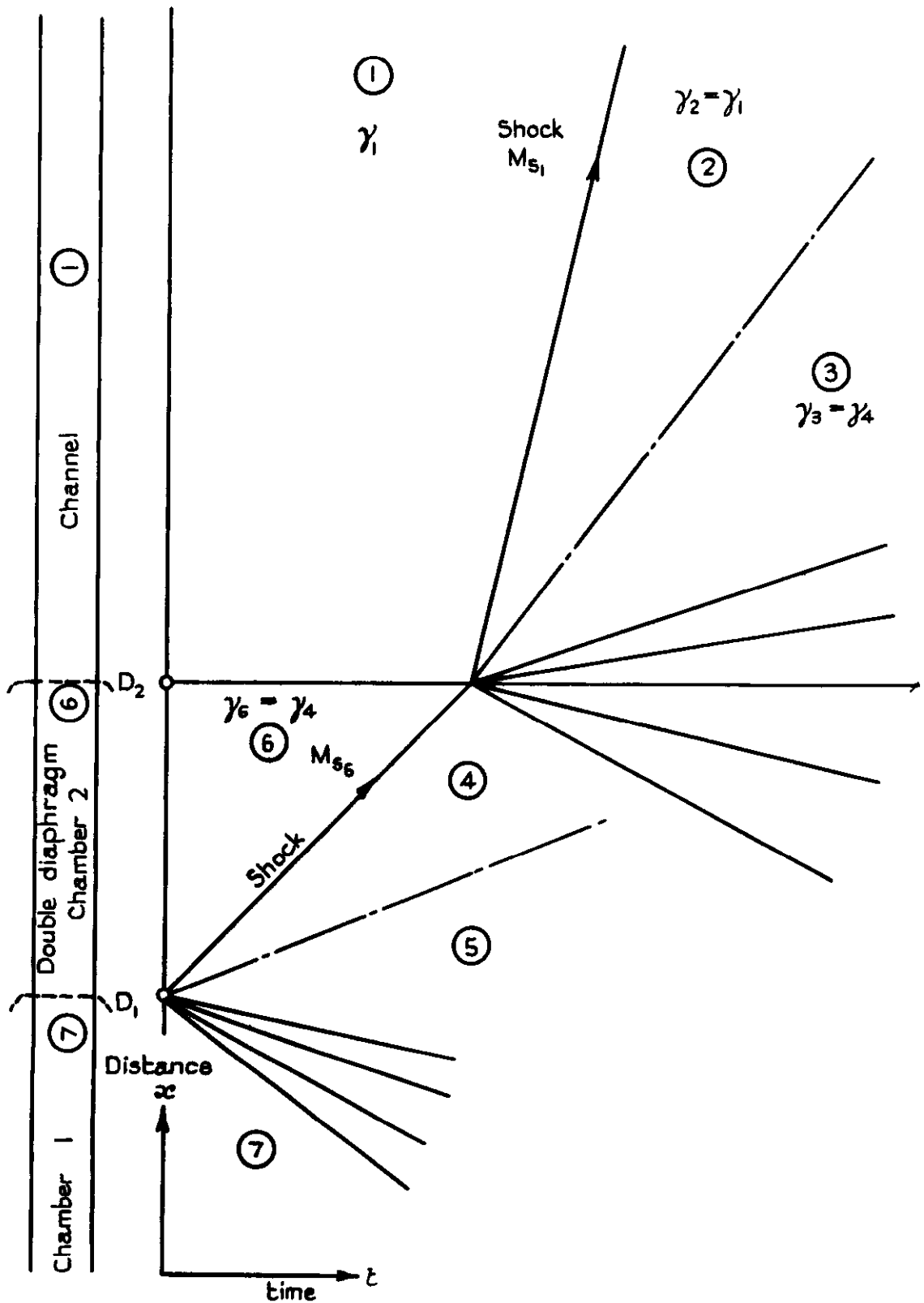


FIG. 4

Double diaphragm shock tube - reflected shock type (see also figure 3)

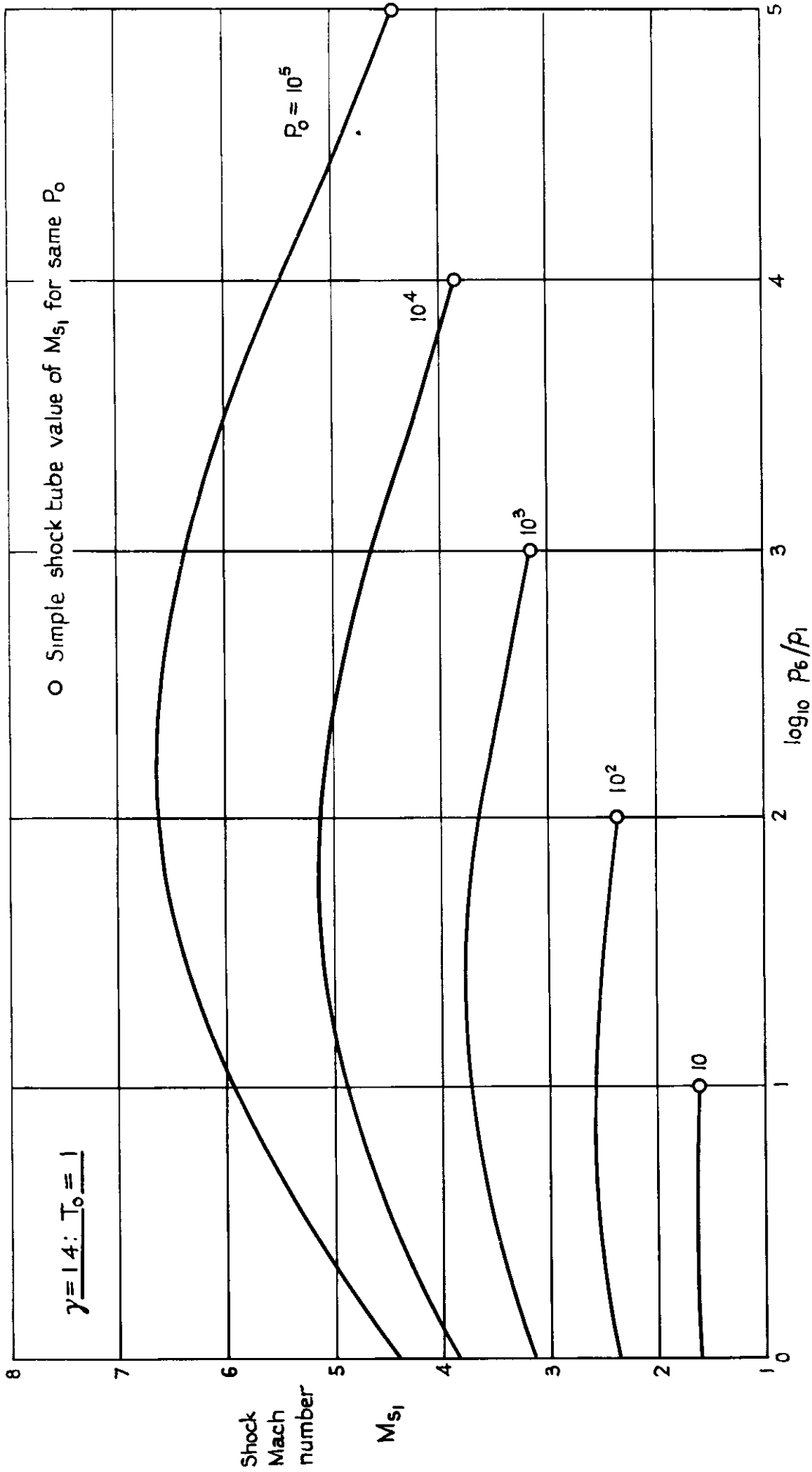
Effect of variation of intermediate pressure p_6 on M_{S_1} for given P_0

FIG. 5.



Double diaphragm shock tube - unsteady expansion type: flow diagram

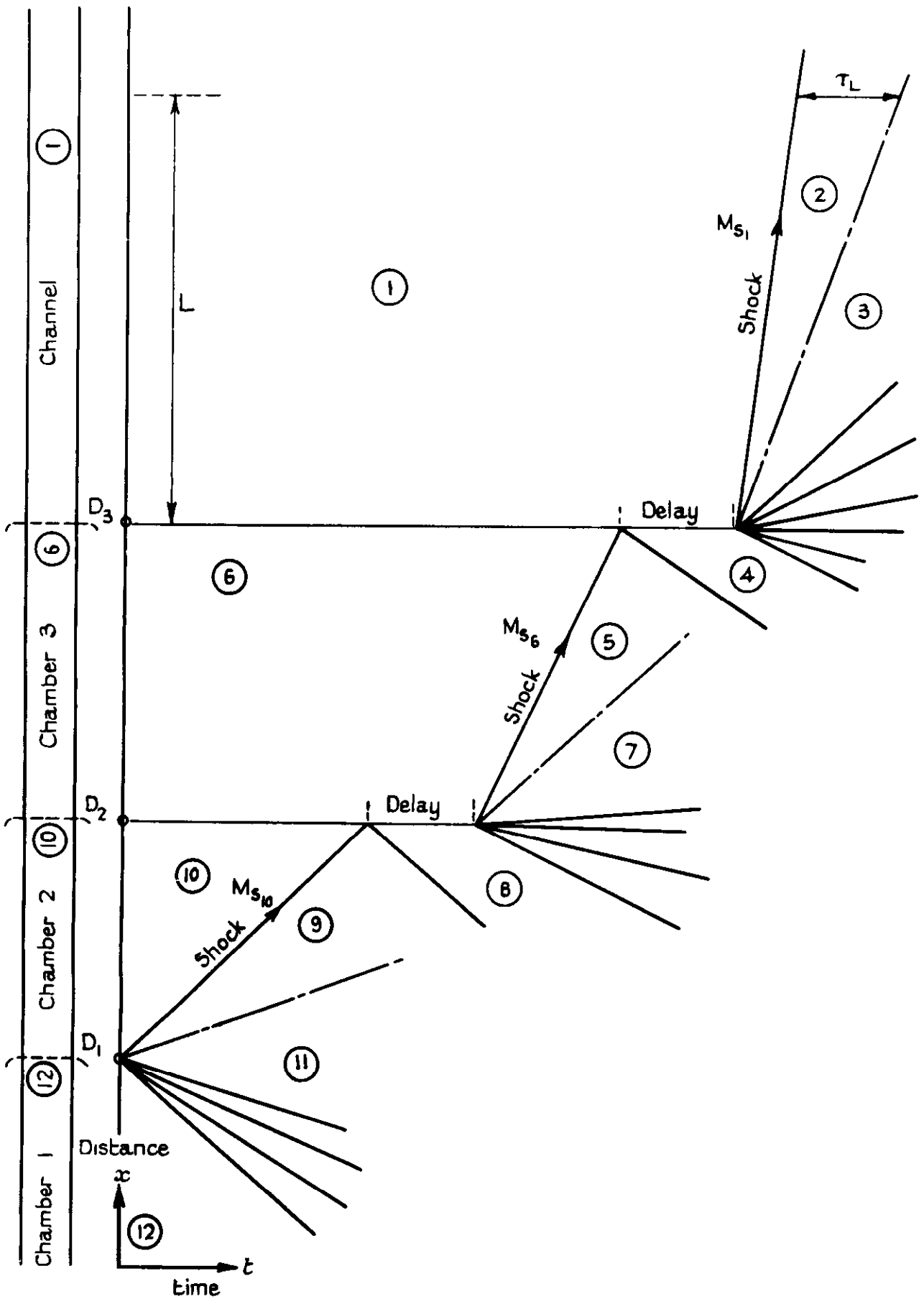
FIG. 6.



Double diaphragm shock tube - unsteady expansion type - (see also figure 5)

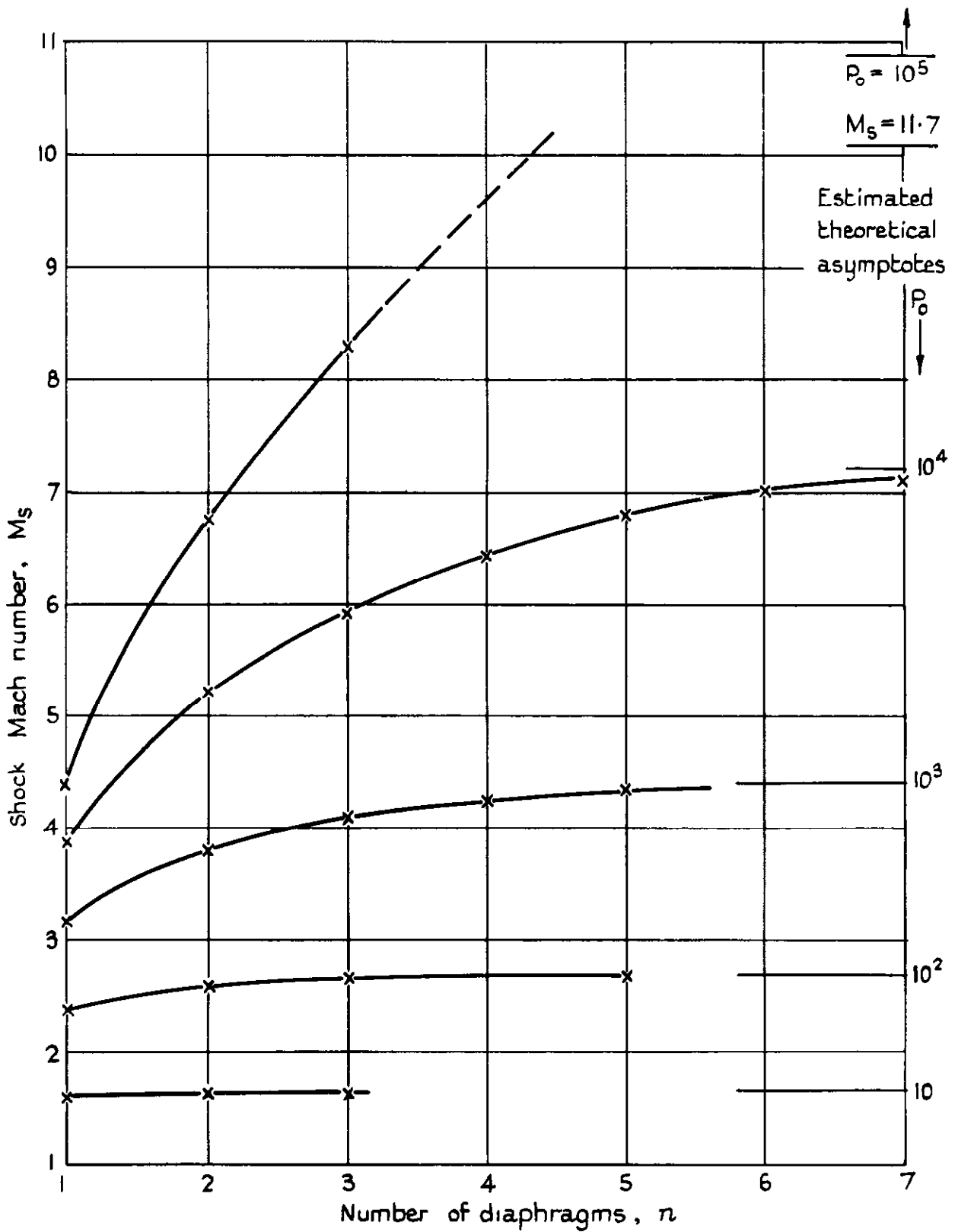
Effect of variation of intermediate pressure P_0 on M_{s1} for given P_6

FIG 7



Multiple diaphragm shock tube - reflected shock type: flow diagram.

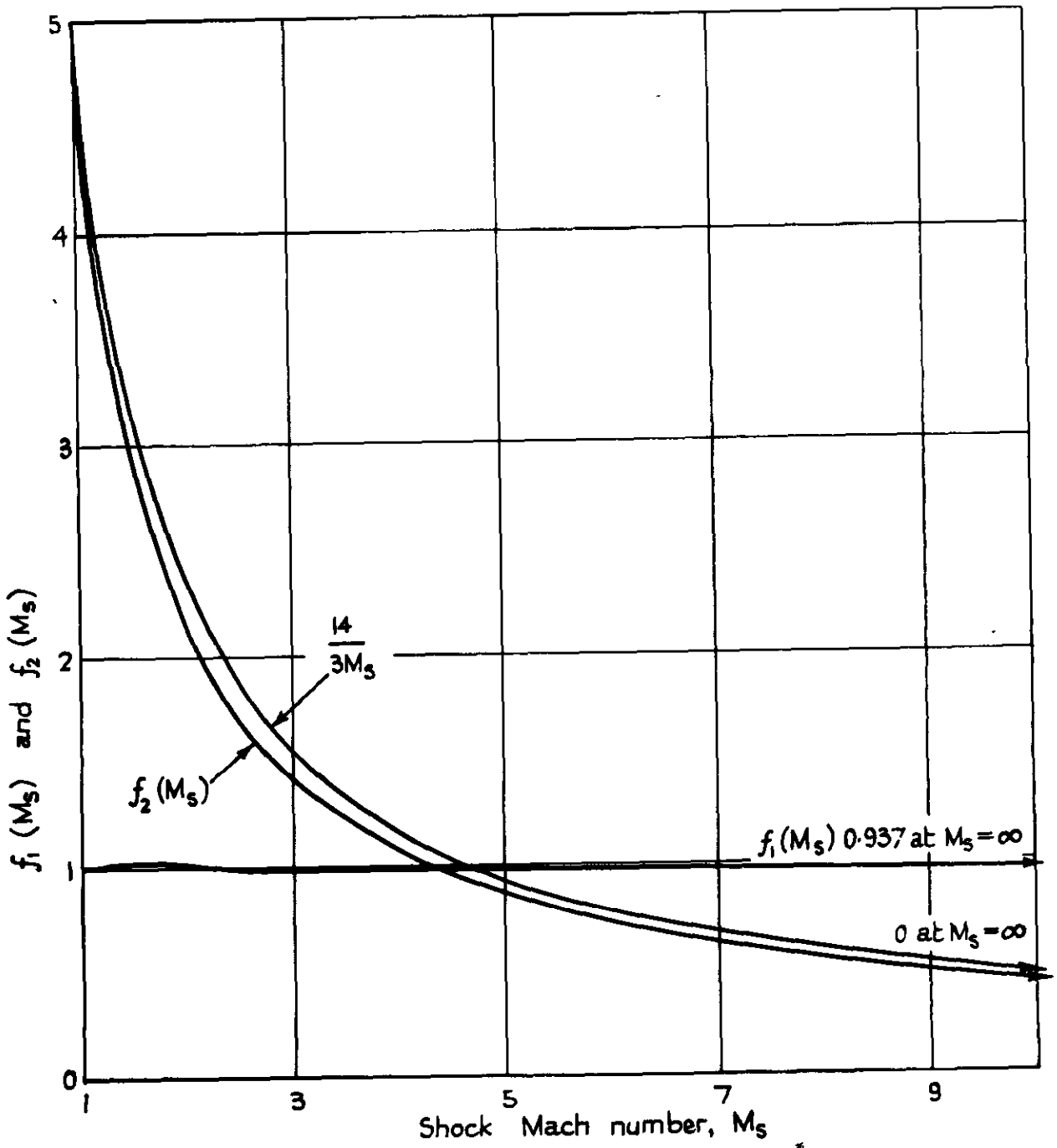
FIG. 8



Multiple diaphragm shock tube - reflected shock type

Influence of number of diaphragms on maximum attainable shock Mach number

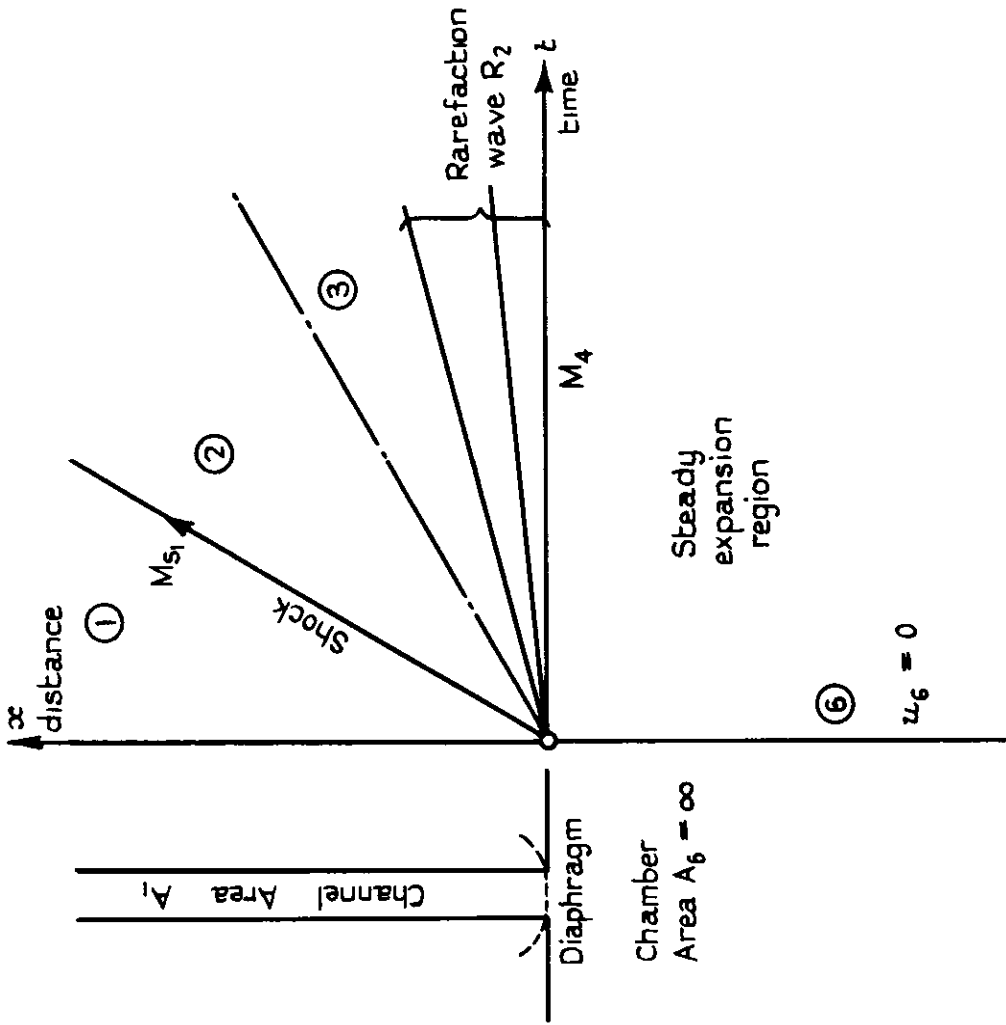
FIG. 9



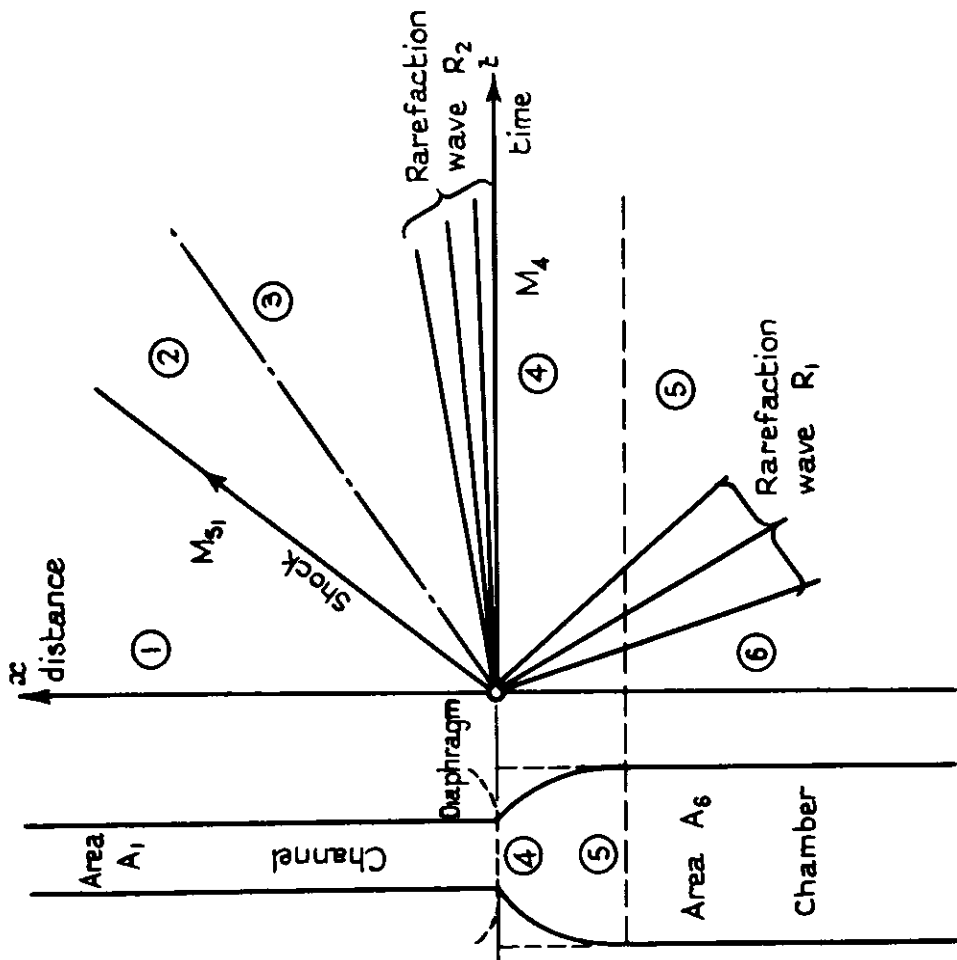
Multiple diaphragm shock tube - reflected shock type.

Functions $f_1(M_s)$ and $f_2(M_s)$

FIG. 10 (a & b)



(a) At the diaphragm section



(b) Area discontinuity at diaphragm station

Shock tubes with area discontinuities

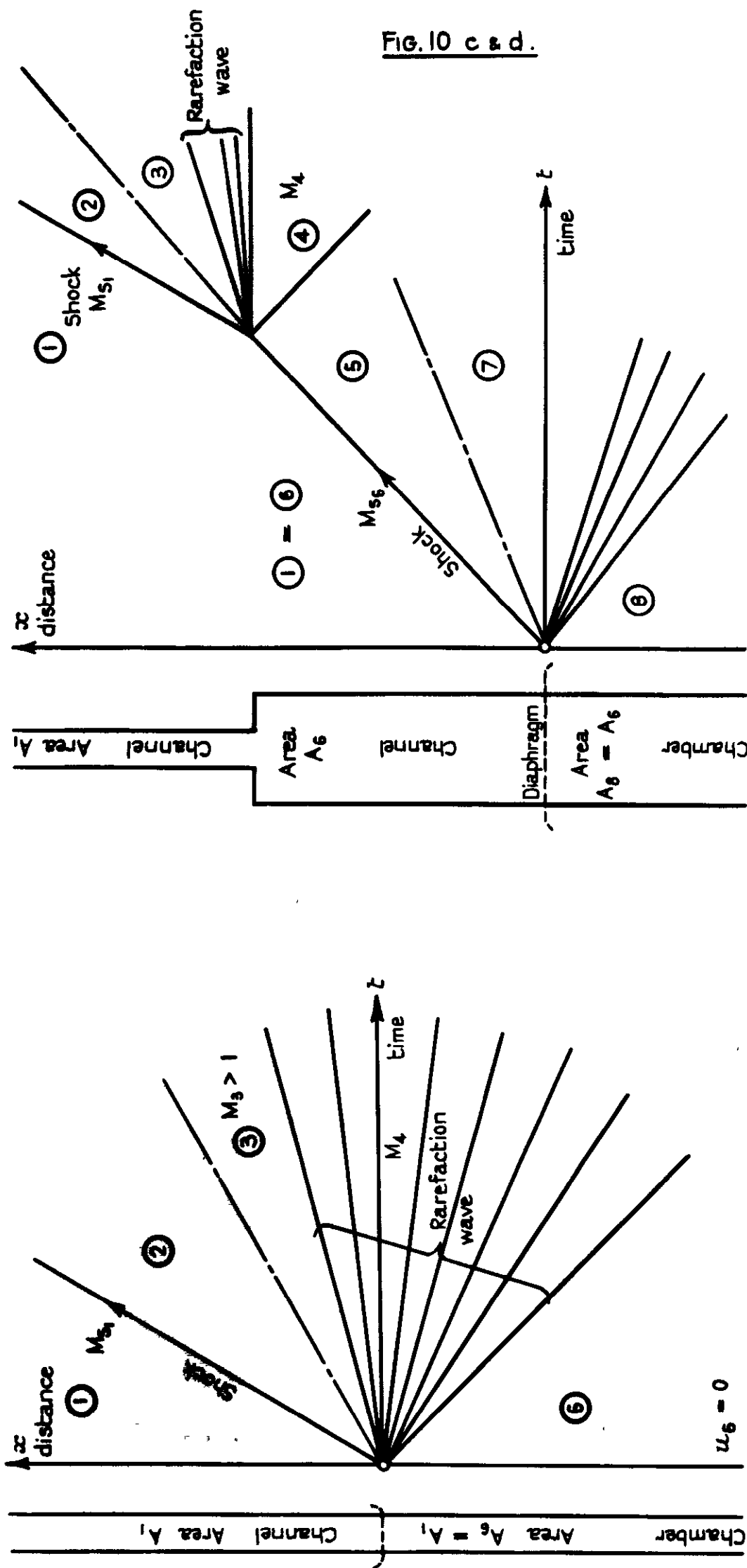


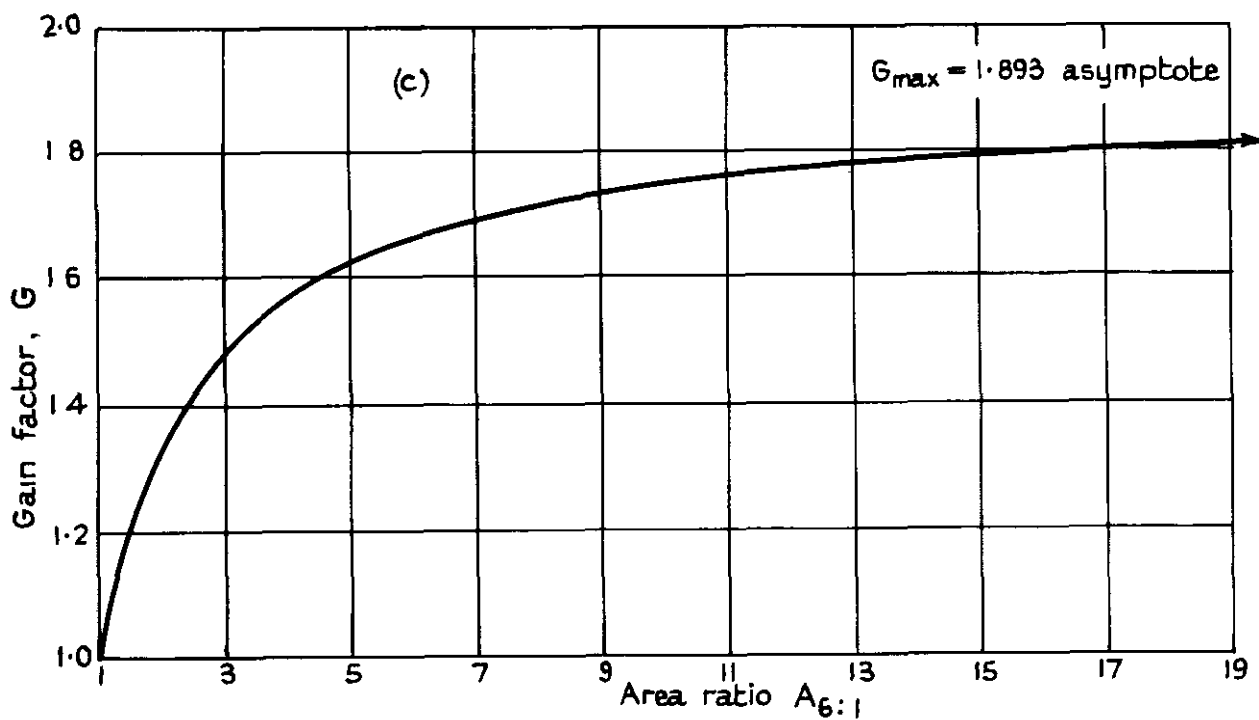
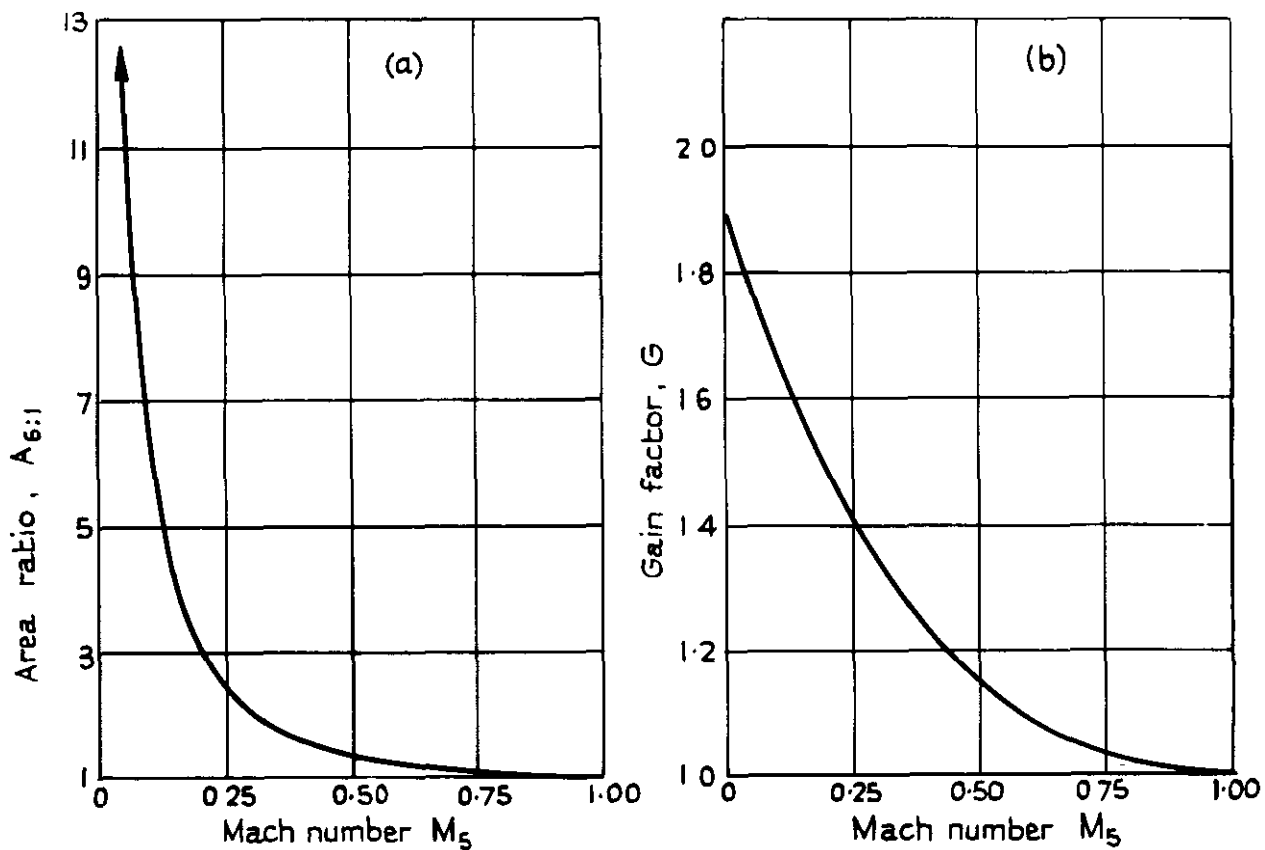
FIG. 10 c & d.

(c) Simple shock tube giving same M_{s1} as fig. 10(b)

(d) At a point along the tube

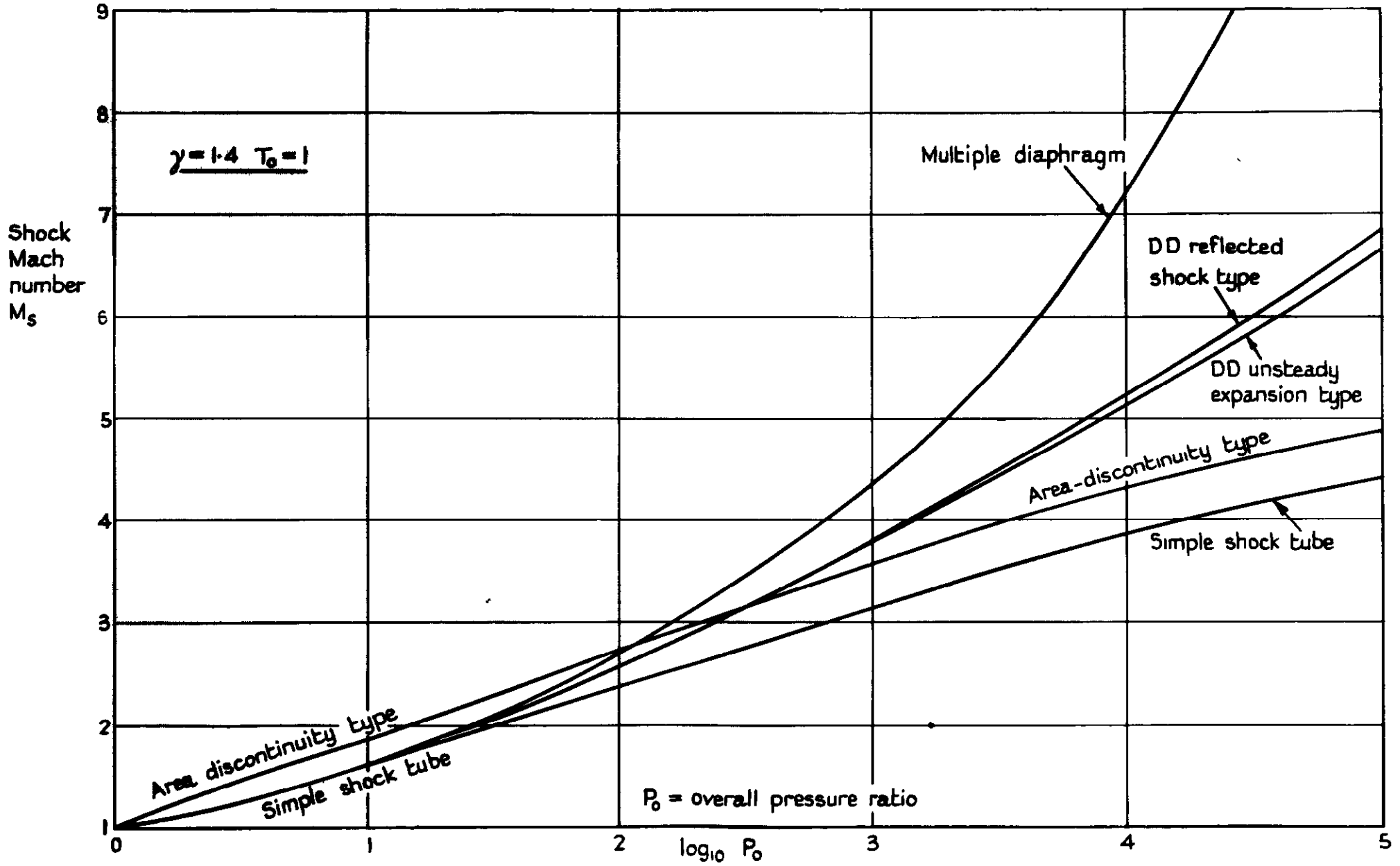
Shock tubes with area discontinuities

FIG. 11.



Shock tube with area discontinuity

Area ratio $A_{6:1}$ and gain factor G - see section 7.1



Comparison of maximum attainable shock Mach number for various types of shock tube

FIG. 12



Crown copyright reserved

Printed and published by
HER MAJESTY'S STATIONERY OFFICE

To be purchased from
York House, Kingsway, London W C 2
423 Oxford Street, London W 1
P O Box 569, London S E 1
13A Castle Street, Edinburgh 2
109 St Mary Street, Cardiff
39 King Street, Manchester 2
Tower Lane, Bristol 1
2 Edmund Street, Birmingham 3
80 Chichester Street, Belfast
or through any bookseller

Printed in Great Britain